154 Lamina cribrosa, angles and blebs
Sunday, May 04, 2014 3:15 PM–5:00 PM
Exhibit/Poster Hall SA Poster Session
Program #/Board # Range: 897–944/A0249–A0296
Organizing Section: Glaucoma

Program Number: 897 **Poster Board Number:** A0249
Presentation Time: 3:15 PM–5:00 PM
***In vivo* examination of lamina cribrosa microarchitecture and optic nerve head morphology in normal human eyes with age**
Amitabha S. Bhakta[1], Nripun Sredar[2], Danica Marrelli[1], Hope M. Queener[1], Jason Porter[1]. [1]College of Optometry, University of Houston, Houston, TX; [2]Department of Computer Science, University of Houston, Houston, TX.
Purpose: Age is a risk factor for the development of glaucoma. Several studies suggest that normal aging could increase the susceptibility of the optic nerve head (ONH) to glaucomatous damage. We examined whether differences exist in lamina cribrosa and ONH structure in vivo between young and older normal subjects.
Methods: Spectral domain optical coherence tomography (SDOCT) [Spectralis HRA+OCT] and adaptive optics scanning laser ophthalmoscope (AOSLO) images of the ONH and anterior lamina cribrosa surface (ALCS) microarchitecture were acquired in eyes of 22 young (20-30 years) and 16 older (≥ 50 years) normal human subjects. ONH features were manually marked in SDOCT radial B-scans to calculate Bruch's membrane opening (BMO) area, mean ALCS depth, mean ALCS radius of curvature (RoC), prelaminar tissue volume (PTV), mean minimum rim width (MRW) and rim volume. Anterior laminar pores were manually marked in AOSLO images and 3D transformed to calculate mean global pore area, elongation and nearest neighbor distance (NND). A Mann-Whitney rank sum test was used to assess statistical differences in all parameters between young and older eyes.
Results: No statistical differences were measured between young and older normal eyes in any ONH or mean global pore parameters. Among the ONH parameters, mean MRW was not significantly reduced in young vs older subjects (317.6 ± 50.0 μm vs 289.8 ± 43.0 μm, P=.08), nor was PTV (1.04 ± 0.16 mm^3 vs 0.95 ± 0.16 mm^3, P=.16). Mean ALCS depth was similar between young (363.9 ± 78.4 μm) and older (352.7 ± 75.71 μm) groups (P=.96), as were BMO area (P=.76), mean RoC (P=.87) and rim volume (P=.51). Mean pore area (young = 2055 ± 561 $μm^2$, older = 2292 ± 744 $μm^2$), elongation (young = 2.06 ± 0.30, older = 2.00 ± 0.30) and NND (young = 75.24 ± 14.5 μm, older = 88.65 ± 25.10 μm) were not significantly different between young and older eyes (P=.39, .37 and .09, respectively).
Conclusions: ONH and mean global laminar pore parameters were similar between our groups of young and older normal eyes. Further analyses are required to determine whether anterior laminar microarchitecture is significantly different on a local scale between age groups. In addition to providing a better understanding of age-related changes in laminar and ONH structure, these normative data will be used for future comparison with values measured in glaucoma patients.
Commercial Relationships: Amitabha S. Bhakta, None; **Nripun Sredar**, None; **Danica Marrelli**, Alcon Laboratories (C), Allergan (C), Allergan (R), Carl Zeiss Meditec (C), Merck (C); **Hope M. Queener**, None; **Jason Porter**, None
Support: NIH Grants R01EY021783 and P30EY07551, University of Houston College of Optometry.

Program Number: 898 **Poster Board Number:** A0250
Presentation Time: 3:15 PM–5:00 PM
Examining *in vivo* changes in predominant lamina cribrosa beam orientation in experimental glaucoma using an automated approach
Nripun Sredar[1], Kevin M. Ivers[2], Hope M. Queener[2], George Zouridakis[1, 3], Jason Porter[2]. [1]Computer Science, Univ of Houston, Houston, TX; [2]College of Optometry, University of Houston, Houston, TX; [3]Engineering Technology, University of Houston, Houston, TX.
Purpose: The lamina cribrosa is suggested to be the initial site of damage to retinal ganglion cell axons in glaucoma. We sought to characterize changes in predominant anterior lamina cribrosa surface (ALCS) beam orientation *in vivo* during the progression of experimental glaucoma (EG).
Methods: We analyzed adaptive optics scanning laser ophthalmoscope (AOSLO) montages of ALCS beams previously acquired in fellow eyes of 4 rhesus monkeys at multiple time-points before and after induction of unilateral experimental glaucoma. AOSLO montages were pre-processed to minimize variations in illumination using a homomorphic filter and contrast-enhanced using a contrast limiting adaptive histogram equalization technique. The predominant orientations of laminar beams throughout a montage were estimated at different overlapping local regions of interest using principal component analysis (PCA). Differences in predominant beam orientation were calculated at corresponding locations over time in control and EG eyes.
Results: The PCA-based method was validated using synthetic data (images of known orientation with different levels of blur and noise) and yielded estimates with small errors in local orientation (0.2 ± 0.2°). The mean difference in local laminar beam orientation across 4 control eyes each assessed at 3 different time-points was low (7.6 ± 1.1°). The mean difference in local beam orientation in EG eyes before the first significant change in beam orientation was 9.3 ± 3.4°. The first time point with a significant change in local beam orientation (mean difference across EG eyes = 38.5 ± 14.7°) coincided with the time of first significant change in manually marked ALCS pore geometry previously reported in these EG eyes. We observed that local predominant beam orientations were mainly radial at baseline, but appeared mainly circumferential at later stages of EG.
Conclusions: The PCA-based method operates directly on *in vivo* grayscale images without the need for binary segmentation, can accurately find local predominant orientation (as indicated by the low errors in synthetic images), and is repeatable (as observed by the low mean differences in control eyes over time). The PCA-based technique can be used to accurately and objectively detect *in vivo* changes in predominant laminar beam orientation in early EG and track longitudinal changes during disease progression.
Commercial Relationships: Nripun Sredar, None; **Kevin M. Ivers**, None; **Hope M. Queener**, None; **George Zouridakis**, None; **Jason Porter**, None
Support: R01 EY021783, P30 EY007551

Program Number: 899 **Poster Board Number:** A0251
Presentation Time: 3:15 PM–5:00 PM
Association between focal lamina cribrosa defects and the parameters of optic disc deformation in glaucomatous eyes with high myopia
Yugo Kimura[1], Masanori Hangai[2], Tadamichi Akagi[1], Munemitsu Yoshikawa[1], Hiroshi Yamada[1], Tomoko Hasegawa[1], Kenji Suda[1], Hanako O. Ikeda[1], Nagahisa Yoshimura[1]. [1]Ophthalmology, Grad Sch of Med, Kyoto Univ, Kyoto, Japan; [2]Ophthalmology, Saitama Medical School Hospital, Saitama, Japan.
Purpose: To investigate whether focal lamina cribrosa (LC) defects are associated with the optic disc deformation in glaucomatous eyes with high myopia
Methods: Three-dimensional images of the optic disc obtained using swept-source optical coherence tomography (SS-OCT) and 6 raster scan images centered at the optic disc by using spectral domain OCT (Spectralis-OCT) were used to evaluate the presence of focal LC defects and Bruch membrane (BM) opening and retinal pigment epithelium (RPE) beginning, respectively. Disc border was determined using infrared images, which automatically corresponded with the raster scan image. The lengths of peripapillary atrophy (PPA) with and without BM were manually measured in each raster scan, and their location was classified into temporal, nasal, superior, and inferior sectors. The tilt angle, which was defined as the angle between the lines connecting both sides of BM opening and both sides of disc border, was measured in the same raster scan images, and the horizontal and vertical tilt angles were examined.
Results: Mean age, spherical equivalent, and mean deviation in Humphrey automated perimetry, respectively, were 49.5 years, -8.4 diopters, and -10.8 dB in 129 glaucomatous eyes with high myopia (< -6 diopters), and 49.4 years, -9.5 diopters, and -1.4 dB in 43 age-matched control subjects with high myopia. Focal LC defects were detected in 70 of the 129 eyes (54.2%) in glaucomatous eyes, which were defined as the LCD(+) group, and no LC defects were detected in the controls. In temporal sector, PPA length without BM was significantly longer in the LCD(+) group (578±338 μm) than in the LCD(-) group (340±316 μm) and control subjects (402±269 μm)($P < 0.001$). PPA length with BM in the temporal sector was not different among the 3 groups. In the nasal, superior, and inferior sectors, PPA length with and without BM was not different among the 3 groups. Horizontal and vertical tilt angles were significantly larger in the LCD(+) group (3.8±3.6° and 9.7±5.7°) than in the LCD(-) group (1.8±2.1° and 5.6±4.7°) and controls (2.3±3.3° and 6.3±5.9°)($P < 0.001$ in both).
Conclusions: The glaucomatous eyes with focal LC defects had longer temporal PPA length without BM and larger tilt angle. Formation of focal LC defects is associated with disc deformation in glaucomatous eyes with high myopia.
Commercial Relationships: Yugo Kimura, None; **Masanori Hangai**, Canon (F), NIDEK (F), Topcon (F); **Tadamichi Akagi**, None; **Munemitsu Yoshikawa**, None; **Hiroshi Yamada**, None; **Tomoko Hasegawa**, None; **Kenji Suda**, None; **Hanako O. Ikeda**, None; **Nagahisa Yoshimura**, Canon (F), NIDEK (F), Topcon (F)

Program Number: 900 **Poster Board Number:** A0252
Presentation Time: 3:15 PM–5:00 PM
Imaging the Lamina Cribrosa using Spectral Domain OCT Enhanced Depth Imaging and Swept Source OCT in Open Angle Glaucoma Patients
Elise Taniguchi, Neha Sangal, Eleftherios I. Paschalis, Louis R. Pasquale, Lucy Q. Shen. Harvard Glaucoma Center of Excellence, Massachusetts Eye and Ear Infirmary, Boston, MA.
Purpose: Swept Source optical coherence tomography (SS-OCT) is a new imaging technology, which has shown promise to visualize the lamina cribrosa (LC), a principal site of glaucomatous optic nerve damage. In this study, we compared SS-OCT to Spectral Domain optical coherence tomography (OCT) with Enhanced Depth Imaging (EDI-OCT) in order to assess inter-observer variability of LC defects in glaucoma patients. Furthermore, we assessed ophthalmic features associated with LC defects detected by both devices.
Methods: 38 eyes of 19 patients with open angle glaucoma underwent radial and horizontal optic nerve serial scans using the EDI-OCT (Heidelberg) and the SS-OCT (Topcon) in a single visit. Two glaucoma specialists performed interpretation of the images and classified eyes into four categories: no defect, pre-laminar defects, focal laminar defects and laminar disinsertions. Disc photographs were used to rule out artifact from vascular shadowing. Characteristics related to glaucoma, such as history of disc hemorrhage, intraocular pressure, Humphrey Visual Field mean deviation, were compared among eyes in those categories. Spearman's rank test was performed for correlated measurements and Kappa agreement was used to assess the inter-observer variability. The one-way analysis of variance test was used to determine clinical factors associated with LC defects.
Results: 32 (84%) serial scans from SS-OCT and 29 (76%) serial scans from EDI-OCT were included in the analysis. The interpretation of the LC images was significantly correlated between the two observers using SS-OCT ($r=0.756, p<0.0001$) and EDI-OCT ($r=0.655, p<0.001$), with comparable inter-observer agreements ($k=0.537$ vs. $k=0.521$, respectively). In 8 (23%) eyes with laminar abnormalities, detected by both observers, the incidence of pre-laminar defect (fig 1A), focal laminar defect (fig 1B) and laminar disinsertion (fig 1C) was 37,5%, 37,5% and 25%, respectively. None of the clinical factors analyzed had correlation with LC abnormalities (ANOVA: $p>0.1$).
Conclusions: Preliminary results suggest that SS-OCT and EDI-OCT images are consistent and both OCTs exhibit good inter-observer agreement when imaging the LC in glaucoma patients. The clinical significance of these defects in glaucoma detection and management remains to be elucidated.

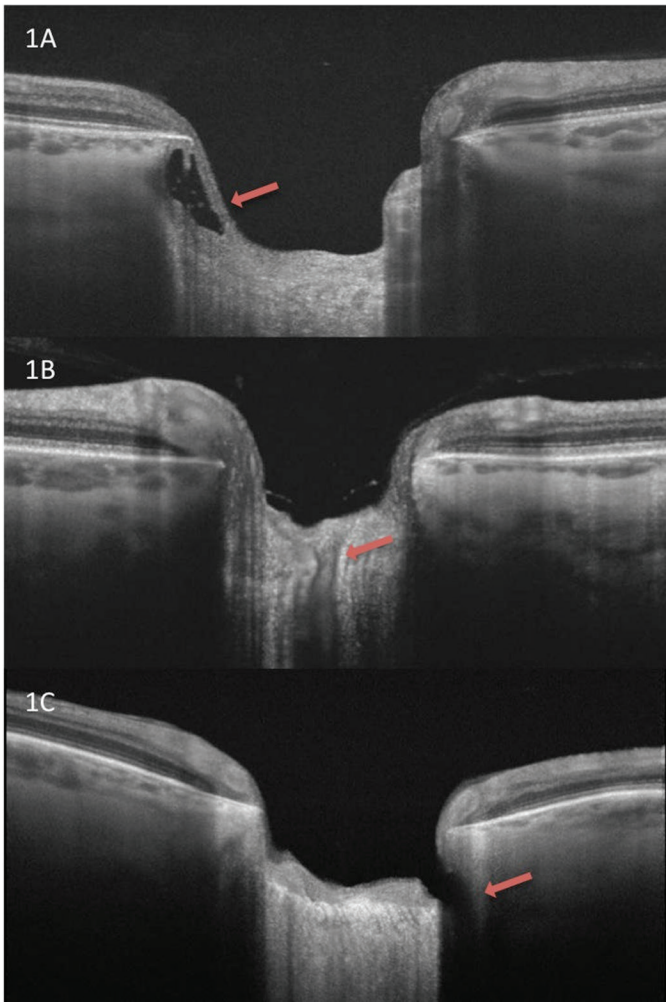

Fig 1.Swept Source OCT.1A-Pre-Laminar Defect,1B-Focal Laminar Defect,1C-Laminar Disinsertion

Commercial Relationships: Elise Taniguchi, None; **Neha Sangal**, None; **Eleftherios I. Paschalis**, None; **Louis R. Pasquale**, None; **Lucy Q. Shen**, None

Support: Miller Research Funds, MEEI; Harvard Glaucoma Center of Excellence, MEEI

Program Number: 901 **Poster Board Number:** A0253
Presentation Time: 3:15 PM–5:00 PM

Evaluation of lamina cribrosa thickness using spectral-domain optical coherent tomography in ocular hypertension

Jong Chul Han, Da Ye Choi, Young Kwun, Changwon Kee. Samsung Medical Center, Seoul, Republic of Korea.

Purpose: To evaluate the difference of lamina cribrosa thickness (LCT) and anterior lamina depth (ALD) between ocular hypertension and normal control

Methods: This was a retrospective case control study comprising 46 ocular hypertension patients and 30 healthy normal control who had undergone enhanced depth imaging optical coherence tomography (EDI-OCT) between Jan 1st and July 31th in 2013. Factors analyzed included age, intraocular pressure (IOP), central corneal thickness (CCT), spherical equivalent, LCT and ALD. Statistical analysis was performed after IOP modification based on the CCT. Provided that 530 μm of CCT is the reference standard of CCT, 3 mmHg per 50 μm of CCT was corrected for IOP modification .

Results: No significant difference was found in IOP, CCT, spherical equivalent, LCT and ALD between ocular hypertension and normal control before and after IOP modification. In case of the patients of ocular hypertension over 24 mmHg, they had significantly thicker lamina cribrosa (258.5 ± 31.8 μm) than normal control (238 ± 28.6 μm) (p =0.04).

Conclusions: Ocular hypertension patients with modified IOP over 24 mmHg have thicker lamina cribrosa thickness than normal control. Thicker LCT may protect the development of glaucoma in ocular hypertension patients.

Commercial Relationships: Jong Chul Han, None; **Da Ye Choi**, None; **Young Kwun**, None; **Changwon Kee**, None

Program Number: 902 **Poster Board Number:** A0254
Presentation Time: 3:15 PM–5:00 PM

Clinical Optic Disc Findings Associated With Focal Lamina Cribrosa Defects in Glaucoma

Mohammed B. Khalil[1], Sung Chul Park[1, 2], Pengcheng Li[1], Christopher C. Teng[1, 2], Jeffrey M. Liebmann[1, 3], Robert Ritch[1, 2].
[1]Moise and Chella Safra Advanced Ocular Imaging Laboratory, New York Eye & Ear Infirmary of the Mount Sinai Health System, New York, NY; [2]Department of Ophthalmology, New York Medical College, Valhalla, NY; [3]Department of Ophthalmology, New York University School of Medicine, New York, NY.

Purpose: To investigate the clinical optic disc findings associated with focal lamina cribrosa defects (FLCD) in glaucoma.

Methods: Serial enhanced depth imaging optical coherence tomography (EDI OCT) B-scans (interval between scans, ~30 μm) of the optic nerve head were obtained from glaucoma patients at various disease stages. EDI OCT scans were reviewed for presence/absence of focal LC defects (laminar holes or disinsertions) by a masked observer. The best quality stereo disc photo taken within 6 months from EDI OCT was selected for each eye by another masked observer. The disc photos were reviewed by another a third masked observer for presence/absence of a notch with remaining neuroretinal rim tissue, a notch with no remaining rim tissue, diffuse rim thinning, bayoneting of circumlinear vessel, beta-zone parapapillary atrophy (PPA), and acquired pit of the optic nerve (APON). Strength of association with the EDI OCT finding (presence/absence of FLCD) was calculated for each of the 6 clinical optic disc findings using Cramér's V test. Disc findings significantly associated with FLCD in Cramér's V test were entered into a multivariable logistic regression model. Disc hemorrhage was not included in the study because it would not be meaningful to include a transient finding such as disc hemorrhage in a cross-sectional analysis of irreversible findings.

Results: 186 eyes of 186 glaucoma patients (mean age, 68±18 years) were included for analysis. A notch with no remaining rim tissue, diffuse rim thinning and APON were significantly correlated with FLCD (all p<0.02), but a notch with remaining rim tissue, beta-zone PPA and bayoneting of circumlinear vessels were not (all p>0.10) (Table 1). In the multivariable logistic regression model, a notch with no remaining rim tissue (p=0.001, odds ratio [OR]=3.47) and APON (p=0.004, OR=10.31) were significantly associated with FLCD. The association between diffuse rim thinning and FLCD was marginally significant (p=0.052 OR=2.26).

Conclusions: A notch with no remaining rim tissue was associated with FLCD, whereas a notch with remaining rim tissue was not. The association between APON and FLCD, previously reported by our group, was confirmed. These clinical optic disc features may be helpful in predicting the presence of FLCD and deciding EDI OCT-guided evaluation of the LC.

Table 1. Clinical Optic Disc Findings versus Focal Lamina Cribrosa Defects (FLCD)

FLCD on EDI OCT	Clinical Optic Disc Findings, Number of Eyes		*P* value (Cramér's *V*)
Notch with Remaining Rim Tissue			
	Absent (N=130)	Present (N=56)	0.102
Absent (N=86)	55	31	(0.120)
Present (N=100)	75	25	
Notch with No Remaining Rim			
	Absent (N=52)	Present (N=134)	**<0.001**
Absent (N=86)	37	49	**(0.311)**
Present (N=100)	15	85	
Diffuse Rim Thinning			
	Absent (N=43)	Present (N=143)	**0.013**
Absent (N=86)	27	59	**(0.182)**
Present (N=100)	16	84	
Bayoneting of Circumlinear Vessel			
	Absent (N=86)	Present (N=100)	0.715
Absent (N=86)	41	45	(0.027)
Present (N=100)	45	55	
Beta-Zone Parapapillary Atrophy			
	Absent (N=67)	Present (N=119)	0.355
Absent (N=86)	34	52	(0.068)
Present (N=100)	33	67	
Acquired Pit of the Optic Nerve			
	Absent (N=167)	Present (N=19)	**<0.001**
Absent (N=86)	84	2	**(0.242)**
Present (N=100)	83	17	

Strength of association: Cramér's *V* >0.5 (high), 0.3-0.5 (moderate), 0.1-0.3 (low), 0-0.1 (little, if any).

Commercial Relationships: Mohammed B. Khalil, None; **Sung Chul Park**, Heidelberg Engineering, GmbH (F), Heidelberg Engineering, GmbH (R); **Pengcheng Li**, None; **Christopher C. Teng**, None; **Jeffrey M. Liebmann**, Heidelberg Engineering, GmbH (C), Heidelberg Engineering, GmbH (F), National Institute of Health (F), New York Glaucoma Research Institute (F); **Robert Ritch**, None
Support: Peter Crowley Research Fund of the New York Eye and Ear Infirmary, HRH Prince Khalid bin Abdullah Al-Saud Research Fund of the New York Glaucoma Research Institute

Program Number: 903 **Poster Board Number:** A0255
Presentation Time: 3:15 PM–5:00 PM
In vivo imaging of lamina cribrosa defects in eyes with distinct patterns of glaucomatous retinal nerve fiber layer damage
KoEun Kim[1, 2], Jin Wook Jeoung[1, 2], Young Kook Kim[1, 2], Bo Ram Seol[1, 2], Ki Ho Park[1, 2], Dong Myung Kim[1, 2]. [1]Ophthalmology, Seoul National University College of Medicine, Seoul, Republic of Korea; [2]Ophthalmology, Seoul National University Hospital, Seoul, Republic of Korea.
Purpose: To investigate the frequency of focal abnormalities in lamina cribrosa (LC) in eyes with distinct patterns of glaucomatous retinal nerve fiber layer (RNFL) damage using swept-source optical coherence tomography (SS-OCT).
Methods: One hundred and ninety-six eyes of 119 subjects with localized RNFL defects, 34 eyes of 23 subjects with diffuse RNFL defects, and 174 eyes of 109 healthy subjects were reviewed. All subjects underwent stereoscopic optic disc photography and in vivo LC imaging using a 3-dimensional optic disc scanning protocol with a prototype SS-OCT (Topcon, Inc., Tokyo, Japan). Two masked graders evaluated serial en face images and 12 radial B-scans to detect focal LC defects.
Results: In eyes with localized RNFL defects, the proportion of eyes with ≥1 LC defect was 61.7%, which was significantly higher than that with diffuse RNFL defects (23.5%) and without any RNFL defects (9.2%; all P <0.001). A total of 187 focal LC defects were found in eyes with localized RNFL defects (1.0 LC defect/eye), 10 in eyes with diffuse RNFL defects (0.3 LC defect/eye), and 17 in healthy eyes (0.1 LC defect/eye).
Conclusions: Focal LC defects were more frequently visible in eyes with localized RNFL defects than those with diffuse RNFL defects. Further investigations are needed to elucidate the pathogenic role of focal LC abnormalities in distinct patterns of glaucomatous RNFL damage.
Commercial Relationships: KoEun Kim, None; **Jin Wook Jeoung**, None; **Young Kook Kim**, None; **Bo Ram Seol**, None; **Ki Ho Park**, None; **Dong Myung Kim**, None

Program Number: 904 **Poster Board Number:** A0256
Presentation Time: 3:15 PM–5:00 PM
Comparison of the anterior lamina cribrosa insertion in patients with open angle glaucoma and healthy subjects
Kyoung Min Lee[1], Eun Ji Lee[1], Tae-Woo Kim[1], Robert N. Weinreb[2]. [1]Ophthalmology, Seoul National University Bundang Hospital, Seongnam, Republic of Korea; [2]Ophthalmology, Hamilton Glaucoma Center, University of Califonia, Sandiego, CA.
Purpose: To determine whether the anterior lamina cribrosa insertion (ALI) is located more posteriorly in open angle glaucoma (OAG) patients than in healthy subjects using swept-source optical coherence tomography (SS-OCT).
Methods: Prospectively, 58 eyes with OAG having inferotemporal wedge shaped retinal nerve fiber layer defect (MD: -4.25 ± 3.55) and 63 healthy eyes were included. Optic disc was imaged by SS-OCT using 12 radial line B-scans centered on the optic disc, each scan at an every half clock hour meridian. ALI depth was assessed at 13 meridians (inferior-temporal-superior) by measuring 2 parameters: 1) ALI position (ALIP) which was defined as the lineal distance from the anterior scleral edge to the ALI, 2) marginal lamina cribrosa depth (MLCD) which was defined as the perpendicular distance from the anterior scleral opening plane to the anterior lamina cribrosa surface at the location of the anterior scleral edge. The two parameters were compared between OAG and healthy eyes at the corresponding meridian.
Results: ALIP was significantly greater in OAG patients at 6.5 and 7 o'clock position (6.5 o'clock: 243 ± 68 μm vs. 205 ± 58 μm, p = 0.002; 7 o'clock: 229 ± 75 μm vs. 176 ± 61 μm, p < 0.001). MLCD was significantly greater in OAG patients at 6 to 7 o'clock and 10.5 o'clock position (6 o'clock: 243 ± 75 μm vs. 186 ± 50 μm, p < 0.001; 6.5 o'clock: 265 ± 88μm vs. 195 ± 53 μm, p < 0.001; 7 o'clock: 248 ± 82 μm vs. 171 ± 59 μm, p < 0.001; 10.5 o'clock: 235 ± 95 μm vs. 182 ± 73 μm, p = 0.001). Baseline intraocular pressure was significantly associated with greater ALIP at 7 o'clock (p = 0.009) and MLCP at 6.5 (p = 0.036) to 7 o'clock (p = 0.003). Age was significantly associated with greater MLCP at 6 o'clock (p = 0.024).
Conclusions: ALI is displaced posteriorly in eyes with OAG compared with healthy eyes, which supports that posterior migration of the lamina cribrosa is a component of optic disc remodeling in glaucoma.

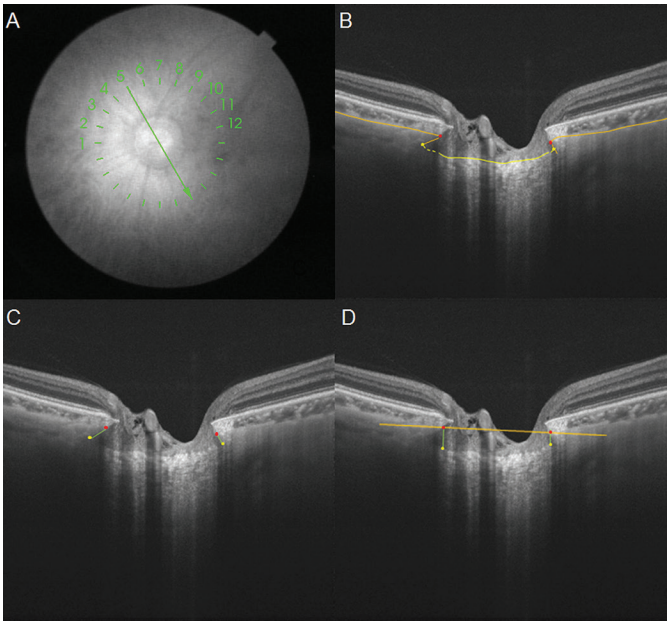

Figure 1. A. 12 radial scans centered on the optic disc. B. Manual delineation of lamina cribrosa and sclera. C. Measurement of ALIP along the scleral canal. D. Measurement of MLCD perpendicular to the scleral opening plane.

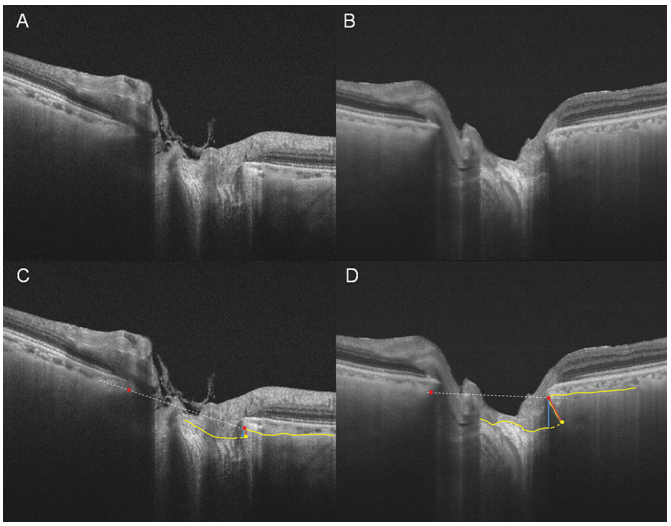

Figure 2. SS-OCT B-scan image of Control (A) and OAG (B) at 7 o'clock meridian. C, D. Manually delineated images of A and B, respectively (yellow lines). Both ALIP (red line) and MLCD (blue line) are increased in OAG (D) than in control (C).

Commercial Relationships: Kyoung Min Lee, None; **Eun Ji Lee**, None; **Tae-Woo Kim**, Topcon (C); **Robert N. Weinreb**, None

Support: Supported by National Research Foundation of Korea Grant funded by Korean Government 2013R1A1A1A05004781

Program Number: 905 **Poster Board Number:** A0257
Presentation Time: 3:15 PM–5:00 PM

Investigating the relationship between focal lamina cribrosa defects and myopia using swept-source optical coherence tomography (SS-OCT)

Bo Ram Seol, Jin Wook Jeoung, Young Kook Kim, Ki Ho Park, Dong Myung Kim. Seoul National University College of Medicine, Seoul, Republic of Korea.

Purpose: To investigate the relationship between focal lamina cribrosa (LC) defects and myopia using swept-source optical coherence tomography (SS-OCT).
Methods: We retrospectively reviewed the medical records of patients who were examined using an SS-OCT system and evaluated myopia-associated factors such as the spherical equivalent (SE) and axial length (AXL). We examined 248 eyes to determine the SE and 124 eyes to determine the AXL. According to the SE value, the 248 eyes were categorized into 2 groups: myopic (109 eyes; <–0.5 diopters) and non-myopic (139 eyes; ≥-0.50 diopters). The myopic group was further classified into 2 groups: moderately myopic (83 eyes; -6.0 to -0.5 diopters) and highly myopic (26 eyes; <-6.0 diopters). According to the AXL value, the 124 eyes were also classified into 2 groups: average (82 eyes; <24.5 mm) and long (42 eyes; ≥24.5 mm); the long group was further classified into 2 groups: medium-long (24 eyes; 24.5–26.0 mm) and very long (18 eyes; ≥26.0 mm). The relationship between focal LC defects and the values of SE and AXL was then evaluated.
Results: Out of the 248 eyes, 66 had focal LC defects. Focal LC defects were more prevalent in eyes of the myopic (P = 0.033) and long (P = 0.008) AXL groups. Furthermore, focal LC defects were found to be more prevalent in the medium-long (50.0%) AXL group than in the very long and average (33.7% and 20.8%, respectively; P = 0.017) groups. Although no statistically significant difference was observed, focal LC defects occurred more frequently in the highly myopic (38.5%) group than in the moderately myopic and non-myopic (31.3%, 21.6%, respectively; P = 0.100) groups.
Conclusions: The SS-OCT imaging demonstrates the 3D structure of LC and allows visualization of focal LC defects. Based on the findings of this study, focal LC defects are significantly associated with myopia.

Commercial Relationships: Bo Ram Seol, None; **Jin Wook Jeoung**, None; **Young Kook Kim**, None; **Ki Ho Park**, None; **Dong Myung Kim**, None

Program Number: 906 **Poster Board Number:** A0258
Presentation Time: 3:15 PM–5:00 PM

Anterior lamina cribrosa morphometrics in myopic glaucoma

Sieun Lee[1], Sherry Han[2], Mei Young[2], Paul Mackenzie[2], Mirza Faisal Beg[1], Marinko V. Sarunic[1]. [1]School of Engineering Science, Simon Fraser University, Burnaby, BC, Canada; [2]Ophthalmology and Visual Science, University of British Columbia, Vancouver, BC, Canada.

Purpose: To investigate anterior laminar shape characteristics in connection with age, axial length, and glaucoma severity among myopic normal and glaucomatous eyes using OCT.
Methods: 32 human eyes from 17 myopic participants (7 normal, 4 unilateral glaucoma, 6 bilateral glaucoma) were imaged using a 1060nm prototype swept-source optical coherence tomography (SS-OCT) system. Bruch's membrane opening (BMO), anterior lamina insertion points (ALIP), and anterior lamina cribrosa surface (ALCS) were manually segmented. Area, eccentricity, and planarity of ALIP were measured by ellipse-fitting. The height, skew, and length of the anterior scleral canal were characterized by vertical, horizontal, and normal distances between BMO and ALIP. ALCS depth was measured from a reference plane fit to ALIP. Multiple regression analysis was performed to assess the effect of age, axial length (AL), and visual field loss quantified by mean deviation (MD). Right eyes (OD, N = 17, 10 normal, 7 glaucomatous) and left eyes (OS, N = 15, 8 normal, 7 glaucomatous) were analyzed separately, along with intereye difference.
Results: The ALIP area was positively correlated with AL (OD: p = 0.0007, OS: p = 0.0270), and ALIP area was significantly larger than BMO area (OD: p = 0.0007, OS: p = 0.0015). ALIP and BMO

ellipses were generally enlongated in the nasal-temporal / superior nasal - inferior temporal direction, and in several cases displayed saddle-like pattern in planarity measurement.
The vertical, horizontal, and normal distance between BMO and ALIP centroids were not significantly correlated with any factor. The canal was consistently skewed toward the nasal direction.
ALCS depth was correlated with MD (OD: p = 0.0001, OS: p = 0.0026), and with AL (OD: p = 0.0012), and in inter-eye difference, with MD only (p = 0.014). ALCS depth was also correlated with Bruch's membrane depth measured on the same datasets in our previous study (OD: p = 0.003, OS: p = 0.043). The intereye difference of ALCS depth was also correlated with the intereye difference of BM depth (p = 0.001).
Conclusions: In the sample of glaucoma patients, posterior bowing of the ALCS is more prominent and significant than overall posterior migration represented by the ALIP position relative to BMO. ALCS shape may be affected by axial length; this is more apparent among normal subjects. Lastly, BM "bowing" or depth (distance of BM surface from a reference plane) is correlated with ALCS depth.

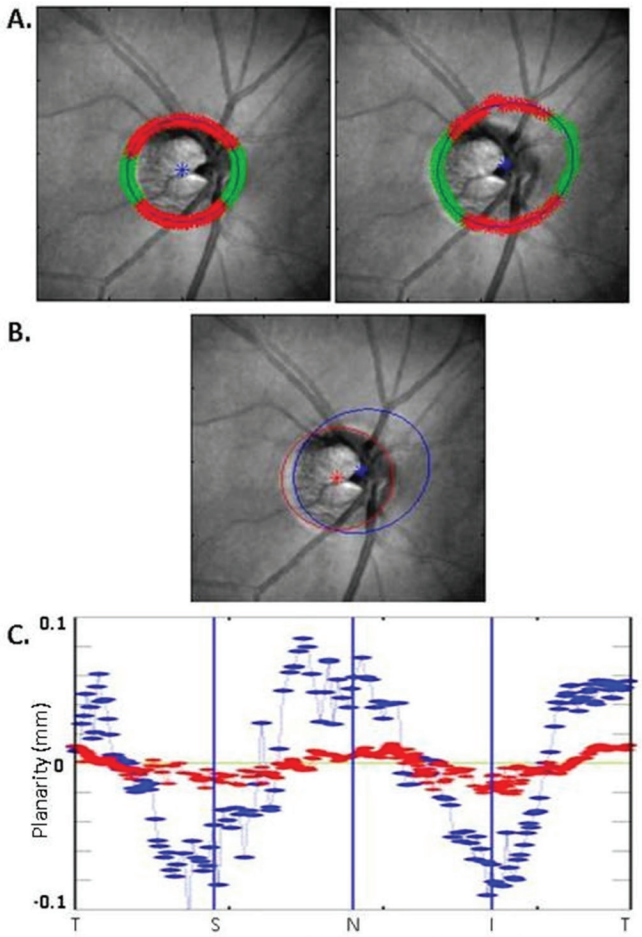

A. Enface OCT image overlay of BMO (left) and ALIP (right). Red indicates anterior to the reference plane, and green indicates posterior to the reference plane. B. BMO (red) and ALIP (blue) position difference viewer from the enface direction. C. Axial distance from the reference plane for BMO (red) and ALIP (blue) delineated points along counter-clockwise direction from temporal (T)) to superior (S), nasal (N), and interior (I) sector.

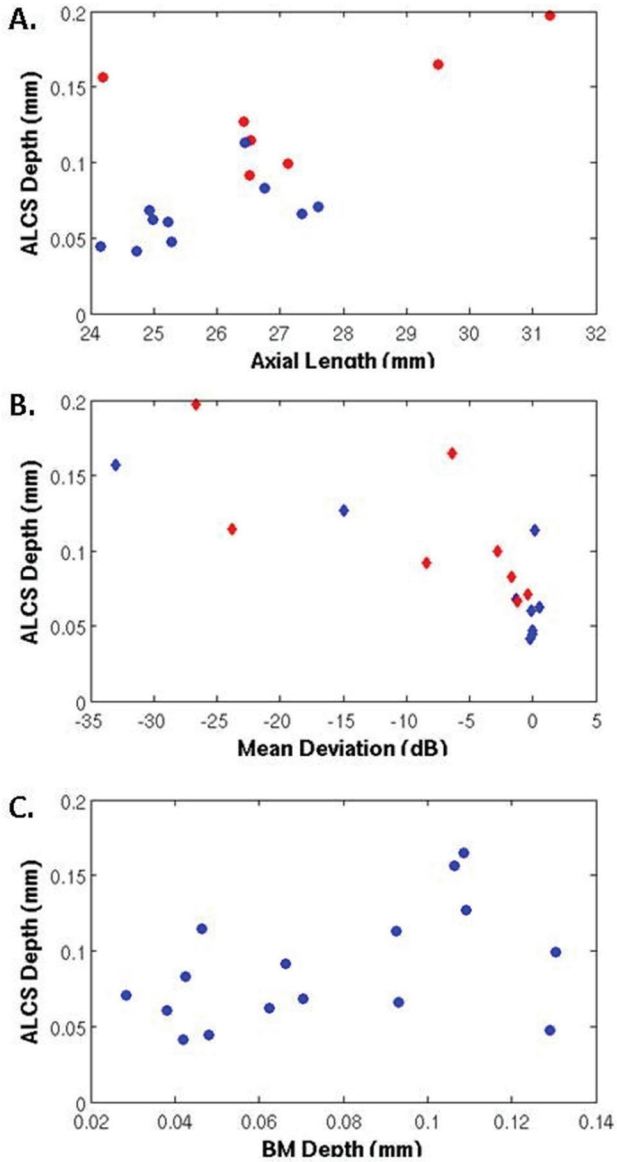

A. ALCS depth vs. axial length. Blue dots are normal eyes, and red dots are glaucomatous eyes. B. ALCS depth vs. mean deviation (dB). Blue diamonds are less myopic eyes (AL < 26.5) and red diamonds are more myopic eyes (AL > 26.5). C. ALCS depth vs. BM depth.

Commercial Relationships: Sieun Lee, None; **Sherry Han**, None; **Mei Young**, None; **Paul Mackenzie**, None; **Mirza Faisal Beg**, None; **Marinko V. Sarunic**, None
Support: MSFHR, CIHR, NSERC

Program Number: 907 **Poster Board Number:** A0259
Presentation Time: 3:15 PM–5:00 PM
CSF Trends in Diseases Associated with Glaucoma
David Fleischman[1], John P. Berdahl[2], Sandra S. Stinnett[3], Michael P. Fautsch[4], R R. Allingham[3]. [1]Ophthalmology, University of North Carolina, Chapel Hill, NC; [2]Vance Thompson Vision, Sioux Falls, SD; [3]Duke University Eye Center, Durham, NC; [4]Ophthalmology, Mayo Clinic, Rochester, MN.
Purpose: Measured cerebrospinal fluid pressure (CSFP) is reduced in patients with POAG compared to non-glaucomatous controls

and may play a role in the pathogenesis of glaucoma. A variety of systemic, vascular and neurologic diseases are associated with glaucoma. In this study, we looked in the Mayo Clinic electronic medical records (EMR) for trends in CSFP in patients with disorders related to risk for POAG.
Methods: All patients having undergone a lumbar puncture (LP) with a CSFP recorded at the Mayo Clinic (Rochester, MN) between 1996-2009 were reviewed. Patients with diagnoses of the following diagnoses were identified: Alzheimer, diabetes, atherosclerosis, hypertension, cerebrovascular accidents, migraine, basal ganglia degeneration, cerebellar degeneration. CSF parameters were compared to the non-diseased groups. Diseases or surgical interventions known to affect CSFP were primary exclusion criteria.
Results: Of 33,932 patients who underwent LP, the Mayo Clinic EMR contained 13,715 patients who met all entry criteria. Significant relative increased CSFP by age was identified in patients with diabetes (20-39 years, +11.71%, $p<0.01$), Alzheimer (>70 years, +6.23%, $p<0.01$), atherosclerosis (20-39 years, +15.48%, $p<0.01$), and hypertension (40-69 years, +2.47%, $p<0.05$). Relative decreased CSFP by age was identified in Alzheimer (40-69 years, -10.56%, $p<0.001$) and cerebellar degeneration (40-69 years, -4.36%, $p<0.01$).
Conclusions: We have found preliminary evidence that CSFP may be altered in several disorders that have a known association with POAG. These include diabetes, systemic hypertension, Alzheimer disease and cerebellar degeneration. The role of CSFP alteration in these disorders, as either a contributing factor or as the result of disease pathology, has received little attention. Alterations of CSFP induced by non-glaucomatous disorders may influence risk for POAG.
Commercial Relationships: David Fleischman, None; **John P. Berdahl**, Alcon (C); **Sandra S. Stinnett**, None; **Michael P. Fautsch**, None; **R R. Allingham**, None
Support: MPF: NIH EY 021727 and Research to Prevent Blindness; Support for RRA, SSS, DF: Research to Prevent Blindness

Program Number: 908 **Poster Board Number:** A0260
Presentation Time: 3:15 PM–5:00 PM
Defects of the lamina cribrosa in myopic eyes with and without glaucoma
Atsuya Miki, Yasushi Ikuno, Tomoko Asai, Shinichi Usui, Kohji Nishida. Ophthalmology, Osaka University Graduate School of Medicine, Suita, Japan.
Purpose: Defects of the lamina cribrosa (LC) are reported to be present in relatively high proportion of glaucomatous eyes whereas rarely observed in normal eyes. Structural vulnerability of the optic nerve is considered as the most probable reason for this preferential laminar damage in glaucomatous eyes. High myopia is also a risk factor for ocular structural vulnerability. The purpose of this study was to evaluate defects of the laminar cribrosa in highly myopic eyes with and without glaucoma, in comparison with healthy control eyes without high myopia.
Methods: Serial horizontal optic disc images were obtained using swept-source optical coherence tomography (SS-OCT) 3D raster scan mode from all eyes. Participants were divided into 3 categories; healthy eyes with neither high myopia nor glaucoma (control group), highly myopic eyes without glaucoma (myopia only group), and highly myopic eyes with glaucoma (myopia and glaucoma group), based on the presence or absence of high myopia (axial length>26.5 mm or spherical equivalent refraction ≤ -6 D) and glaucomatous optic neuropathy. Focal LC defects were identified using a standardized protocol by a grader masked to clinical information.
Results: A total of 118 eyes (83 subjects) were examined, including 20 control eyes (12 subjects), 32 myopia only eyes (27 subjects), and 66 myopia and glaucoma eyes (44 subjects). Focal LC defects were observed in 1 eye (5%) in the control group, 6 eyes (18.8%) in the myopia only group, and 27 eyes (40.9%) in the myopia and glaucoma group. The proportion of having at least one LC defect was significantly different between groups ($P=0.0032$, Chi-square test).
Conclusions: Highly myopic eyes without glaucoma showed an increased risk of having a LC defect compared with control eyes. Glaucoma further increased the risk of laminar abnormality. The existence of the LC damage in highly myopic eyes without glaucoma may suggest the risk of future retinal nerve fiber layer damage in those eyes and at least partly explain the increased risk of developing glaucoma in myopic eyes.
Commercial Relationships: Atsuya Miki, NIDEK (C); **Yasushi Ikuno**, Tomey (F), Topcon (F); **Tomoko Asai**, None; **Shinichi Usui**, None; **Kohji Nishida**, None

Program Number: 909 **Poster Board Number:** A0261
Presentation Time: 3:15 PM–5:00 PM
Assessment of Lamina cribrosa related parameters for the diagnosis of glaucoma and prediction of progression
Kyung Rim Sung, In Kyun Hahn, Ho Seok Chung. Ophthalmology, Asan Medical Center, University of Ulsan, Seoul, Republic of Korea.
Purpose: Lamina cribrosa (LC) of the optic nerve head has been considered as primary site for glaucoma pathogenesis. LC thickness determined by optical coherence tomography (OCT) was decreased in glaucomatous eyes, so it can be a potential marker for glaucoma diagnosis. Thus, we intended to evaluate the characteristics of LC related parameters in normal and glaucomatous eyes with wide range of axial length (AXL) and the baseline LC thickness measurement can predict future progression of glaucoma.
Methods: LC and prelamina thickness were determined by Spectralis OCT enhanced depth imaging mode. Eyes were divided into three groups according to AXL, longer (26mm>), mid-level (23-26mm), and shorter (23mm) groups in each normal and glaucomatous eyes. Glaucoma diagnostic capability of LC related parameters was evaluated by area under the receiver operating characteristic curve (AUC). Glaucomatous subjects followed longer than 2 years from baseline LC measurement were also analyzed. Cox proportional hazard model was used to find putative factors associated with glaucoma progression.
Results: Total 410 subjects (glaucoma; 240, normal; 170) were included. Overall, LC was significantly thinner in eyes with longer AXL than those with shorter AXL. In eye with mid-level AXL, glaucomatous eye showed significantly lower LC thickness than normal group ($p<0.002$), but no difference between normal and glaucomatous eyes in both eyes with longer and shorter AXL ($p=0753$, 0.212, respectively). Thus, AUCs for discrimination between normal and glaucomatous eyes were generally lower in eyes with longer and shorter AXL groups (0.533-0.678). Among 120 subjects who were followed more than 2 years after baseline LC measurement, 35 eyes showed glaucoma progression. Average retinal nerve fiber layer, LC and prelamina thicknesses were significantly associated with glaucoma progression (Hazard ratio; 0.973, 0.979, and 0.993, $p=0.008$, 0.011, and 0.035, respectively).
Conclusions: LC thickness determined by OCT showed possibility of glaucoma progression prediction. In the mean time, eyes with longer and shorter AXL, LC thickness did not show good diagnostic capability for glaucoma. Thus, when using LC related parameters for glaucoma diagnosis, the result should be interpreted with caution considering AXL. Our result also suggests that glaucomatous LC change may be differently manifested in eyes with different AXL.
Commercial Relationships: Kyung Rim Sung, None; **In Kyun Hahn**, None; **Ho Seok Chung**, None

Support: This study was supported by a grant (2013-0513) from the Asan Medical Center, Seoul, Korea.

Program Number: 910 **Poster Board Number:** A0262
Presentation Time: 3:15 PM–5:00 PM
***In vivo* changes in local lamina cribrosa microarchitecture and optic nerve head structure in early experimental glaucoma**
Kevin M. Ivers[1], Nripun Sredar[2], Nimesh B. Patel[1], Lakshmi Rajagopalan[1], Hope M. Queener[1], Ronald S. Harwerth[1], Jason Porter[1]. [1]College of Optometry, University of Houston, Houston, TX; [2]Department of Computer Science, University of Houston, Houston, TX.
Purpose: The purpose of the current study was to examine local vs. global changes in anterior lamina cribrosa surface (ALCS) pores and their association with optic nerve head (ONH) and retinal nerve fiber layer thickness (RNFLT) changes *in vivo* in early experimental glaucoma (EG).
Methods: Spectral domain optical coherence tomography (SDOCT) images (48, 20° radial B-scans; Spectralis HRA+OCT) centered on the ONH were acquired before and approximately every 2 weeks after inducing unilateral EG in 5 rhesus monkeys. Mean ALCS depth (ALCSD) and minimum rim width (MRW) were quantified from manually segmented radial scans. RNFLT was calculated from SDOCT 12° circular scans. Adaptive optics scanning laser ophthalmoscope (AOSLO) images of ALCS pores were acquired at all time-points. Mean ALCS pore area, elongation, and nearest neighbor distance (NND) were quantified globally, in 60° sectors, and in central and peripheral regions from 3D transformed AOSLO images.
Results: At the first time of change in ALCS pores in EG eyes, mean pore area increased globally (18.3±13.4%, P<.05), and locally in the temporal sector (33.9±15.8%, P<.05) and peripheral region (4 of 5 eyes). Mean pore NND also increased significantly across eyes in the peripheral region (21.3±13.9%, P<.05). Local changes in one or more pore parameters were measured in 3 of 5 eyes prior to a globally measured change in the same parameter. When examining laminar and ONH structural change in early EG (i.e., first change in global or local pore parameters, ALCSD, MRW or RNFLT from baseline), simultaneous changes in mean ALCSD, local pore geometry, and mean MRW occurred prior to RNFLT loss in 3 eyes. Simultaneous changes in mean ALCSD and laminar pore geometry occurred prior to a concurrent change in mean MRW and RNFLT in 1 eye, while simultaneous changes in mean ALCSD and MRW occurred prior to laminar pore and subsequent RNFLT changes in 1 eye.
Conclusions: A change in mean ALCSD always occurred first in early EG and preceded or occurred simultaneously with the first change in mean MRW and laminar pore geometry (measured globally or locally). The increased sensitivity afforded by a local vs. global quantification of laminar pores can enable earlier detection of laminar pore change and provide insights on biomechanical changes in laminar microarchitecture *in vivo* in early glaucoma.
Commercial Relationships: Kevin M. Ivers, None; **Nripun Sredar**, None; **Nimesh B. Patel**, None; **Lakshmi Rajagopalan**, None; **Hope M. Queener**, None; **Ronald S. Harwerth**, None; **Jason Porter**, None
Support: NIH Grants R01 EY021783, K23 EY021761, R01 EY001139, and P30 EY007551

Program Number: 911 **Poster Board Number:** A0263
Presentation Time: 3:15 PM–5:00 PM
In Vivo Three-Dimensional Lamina Cribrosa (LC) Microarchitecture in Healthy Subjects Using Adaptive Optics Spectral-Domain Optical Coherence Tomography (AO-SDOCT)
Zach Nadler[1], Bo Wang[1, 2], Gadi Wollstein[1], Daniel D. Ferguson[3], Ankit Patel[3], Daniel X. Hammer[4], Hiroshi Ishikawa[1, 2], Ian A. Sigal[1, 2], Larry Kagemann[1, 2], Joel S. Schuman[1, 2]. [1]UPMC Eye Center, Ophthalmology and Visual Science Research Center, Department of Ophthalmology, University of Pittsburgh School of Medicine, Pittsburgh, PA; [2]Department of Bioengineering, Swanson School of Engineering, University of Pittsburgh, Pittsburgh, PA; [3]Physical Sciences Inc., Andover, MA; [4]Center for Devices and Radiological Health, Food and Drug Administration, Silver Spring, MD.
Purpose: To characterize the in vivo 3D LC microarchitecture of healthy eyes using AO-SDOCT.
Methods: A multimodal retinal imaging system (Physical Sciences Inc, Andover, MA) which includes AO-SDOCT with a 1050nm light source and AO confocal scanning laser ophthalmoscopy (AO-CSLO) was used in this study. One randomly selected eye from each of 32 healthy subjects was scanned in a 6°x6° window centered on the LC. Subjects also underwent scanning with Cirrus HD-OCT (Zeiss, Dublin, CA). Scans with poor scan quality or movement artifact were excluded from analysis. LC microarchitecture was semi-automatically segmented and quantified for beam and pore structure using a previously described method (PMID: 24298418). Disc delineations automatically output from Cirrus scans were used to divide the LC into quadrants and into central and peripheral regions of equal areas. Microarchitecture was also considered with depth by dividing the LC into anterior, middle, and posterior thirds. A paired t-test weighted by the fraction of LC visible was used to compare structure between regions.
Results: The study population included 18 females and 14 males (18 OD, 14 OS) with a mean age of 40.7±16.9 years. After quality exclusion, 17 eyes qualified for analysis (53.1%). LC microarchitecture measurements are summarized in the Table. The nasal quadrant was excluded due to poor visualization. The central sector showed greater connective tissue volume fraction (CTVF) and thicker beams as compared to the periphery. There was no statistically significant difference between superior and inferior quadrants. Both superior and inferior quadrants showed greater CTVF, beam thickness and pore thickness than the temporal quadrant. CTVF decreased at greater depths ($p<0.05$), while the middle third showed the greatest beam thickness ($p<0.01$).
Conclusions: In vivo analysis of healthy eyes using AO-SDOCT showed significant, albeit small, regional variation in LC microarchitecture by quadrant, radially, and with depth, which should be considered in further studies of the LC.

	Overall	Central	Peripheral	Superior	Temporal	Inferior
CTVF (%)	69.6	69.9✦	68.6✦	70.0★	69.1★	70.1
Beam Thickness (μm)	38.1	38.9✦	35.3✦	39.3★	37.2★	38.4
Pore Diameter (μm)	28.0	28.5	26.5	29.7★	27.1★	28.8
Pore Area (μm²)	1308	1348	1206	1356	1290	1337
Visualized Tissue (%)	21.6	33.3	10.7	18.3	56.5	11.1

Matching symbols indicate statistically significant difference between regions

Regional measurement means for LC microarchitecture
Commercial Relationships: Zach Nadler, None; **Bo Wang**, None; **Gadi Wollstein**, None; **Daniel D. Ferguson**, Physical Sciences Inc. (E); **Ankit Patel**, Physical Sciences Inc. (E); **Daniel X. Hammer**, Physical Sciences Inc (C); **Hiroshi Ishikawa**, None; **Ian A. Sigal**, None; **Larry Kagemann**, None; **Joel S. Schuman**, Zeiss (P)

Support: National Institute of Health contracts R01EY013178, R44EY018986, P30EY008098 (Bethesda, MD) The Eye and Ear Foundation (Pittsburgh, PA) and unrestricted grants from Research to Prevent Blindness (New York, NY).

Program Number: 912 **Poster Board Number:** A0264
Presentation Time: 3:15 PM–5:00 PM
Visibility of the Lamina Cribrosa Using OCT: A Comparison of Devices and Techniques

Nicholas G. Strouthidis[1, 2], Sanchalika Acharyya[3], Tin A. Tun[2, 4], Rahat Husain[2, 4], Benjamin A. Haaland[3, 5], Wei Xin[4], Jean M. Mari[6], Shamira Perera[2, 4], Tin Aung[2, 4], Michael J. Girard[2, 7]. [1]NIHR Biomedical Research Centre at Moorfields Eye Hospital NHS Foundation Trust and UCL Institute of Ophthalmology, London, United Kingdom; [2]Singapore Eye Research Institute, Singapore, Singapore; [3]Centre for Quantitative Medicine, Duke NUS Graduate Medical School, Singapore, Singapore; [4]Singapore National Eye Centre, Singapore, Singapore; [5]Department of Statistics and Applied Probability, National University of Singapore, Singapore, Singapore; [6]Department of Medical Physics and Bioengineering, UCL, London, United Kingdom; [7]Department of Biomedical Engineering, National University of Singapore, Singapore, Singapore.

Purpose: To compare lamina cribrosa (LC) visibility and interobserver agreement, in images acquired from glaucoma and normal subjects using 3 OCT devices, with and without enhanced depth imaging (EDI) and with adaptive compensation (AC).

Methods: 60 glaucoma and 60 control subjects were imaged using Spectralis and Cirrus OCT devices both with and without EDI, and using the DR1 OCT. A horizontal B-scan was acquired through the disc center (40X scan averaging for Spectralis/Cirrus, 32X for DR1). AC was applied to reduce light attenuation and improve LC visibility (Mari, et al. IOVS 2013). A subjective grading system was designed to assess visibility of anterior and posterior LC surfaces, and LC/sclera insertions. Two expert observers (NGS, MJAG) graded the 1200 images in a randomized sequence, masked to diagnosis, device or technique. LC visibility was confined to a region limited by Bruch's Membrane Opening. Anterior LC was graded 0 (not visible), 1 (< 25% visible), 2 (25-50%), 3 (50-75%) and 4 (>75%), posterior LC either 0 (not visible) or 1 (any region visible), and LC insertions 0 (none visible), 1 (1 insertion visible), or 2 (both visible). The effect of EDI or AC was assessed using generalized estimating equations. Visibility grades were compared using pairwise Wald tests. Agreement between observers was assessed using weighted kappa.

Results: AC improved anterior LC visibility for any device independent of EDI. DR1 + AC and Cirrus + EDI + AC generated the highest mean grades (both 3.04), significantly better than other methods ($p < 0.05$). DR1 + AC was the best performing method (mean 1.12) for LC insertion visibility. Posterior LC visibility was poor regardless of method. For all LC structures, interobserver agreement was fair-moderate (kappa score range 0.45 - 0.5). No variable was associated with increased anterior LC visibility, anterior chamber depth increased LC insertion visibility for Spectralis + EDI + AC and IOP was associated with expert agreement for anterior LC for Spectralis + EDI + AC (all $p < 0.05$).

Conclusions: Applying AC, independent of EDI, outperforms standard methods for anterior LC or LC insertion visibility. Posterior LC visibility remains poor suggesting that LC thickness measurements are unreliable at present. Fair to moderate interobserver agreement suggests that caution is required when interpreting LC images, although application of AC can improve LC detection.

Commercial Relationships: Nicholas G. Strouthidis, None; **Sanchalika Acharyya**, None; **Tin A. Tun**, None; **Rahat Husain**, None; **Benjamin A. Haaland**, None; **Wei Xin**, None; **Jean M. Mari**, None; **Shamira Perera**, None; **Tin Aung**, CZM (F), CZM (R); **Michael J. Girard**, None

Program Number: 913 **Poster Board Number:** A0265
Presentation Time: 3:15 PM–5:00 PM
In vivo Visualization of Posterior Lamina Cribrosa (LC) using SD-OCT Validated with Histology

HUONG TRAN[1, 2], Bo Wang[1, 2], Ning-Jiun Jan[1, 2], Gadi Wollstein[2], Matthew A. Smith[2], Larry Kagemann[1, 2], Hiroshi Ishikawa[1, 2], Joel S. Schuman[1, 2], Elizabeth Tyler-Kabara[1, 3], Ian A. Sigal[1, 2]. [1]Bioengineering, University of Pittsburgh, Pittsburgh, PA; [2]UPMC Eye Ctr/Eye and Ear Inst/Ophthal, University of Pittsburgh School of Medicine, Pittsburgh, PA; [3]Neurological Surgery, University of Pittsburgh, Pittsburgh, PA.

Purpose: The LC plays a central role in the pathophysiology of glaucoma, and therefore its visualization has great potential to help understand the disease. Spectral domain (SD-) OCT has been demonstrated suitable to visualize the anterior surface of the LC in vivo, but the visibility of the posterior LC remains controversial. Our goal was to test the hypothesis that SD-OCT allows visualization of the posterior LC consistently across scans and eyes, and with sufficient quality to discern the microstructure of even the most posterior LC.

Methods: Eyes from two monkeys were cannulated and IOP was controlled using gravity perfusion. One eye from each monkey was scanned three times using OCT (Bioptigen, 3mm x 3mm, 512 x 512 pixels). Following this, both eyes were enucleated and perfusion fixed at an IOP of 30mmHg, 30 minutes post-death. They were then cryosectioned and imaged with a stereomicroscope (Nikon SMZ1500, 16bit greyscale, 0.765μm/pixel). The OCT-scanned eyes were sectioned coronally to verify the OCT-histology correspondence of LC microstructure. The non-OCT-scanned eyes were sectioned sagittally to evaluate the penetration depth of OCT signal. We delineated the visible posterior LC every 8th B-scan and computed the fraction of the scleral canal (defined by Bruch's membrane opening - BMO). We performed the delineation in the three scans from each monkey, and the results compared to determine the repeatability of LC visibility.

Results: Histology confirmed that the most posterior LC was visible in the OCT images (Figure). Qualitative comparison shows correspondence in LC microstructure between OCT and histology (Figure). Quantitative analysis shows comparable LC thickness: 335±4μm for OCT and 330±30μm for histology. Using BMO plane as a reference, the fraction of visible posterior LC was approximately 50% and was consistent within the three OCT scans from each monkey (Table).

Conclusions: SD-OCT allows visualization of the entire monkey LC thickness in vivo including the most posterior pores and beams. Posterior LC was consistently identified in approximately half of the area of the scleral canal defined by BMO. The extent to which our results apply to humans remains to be determined.

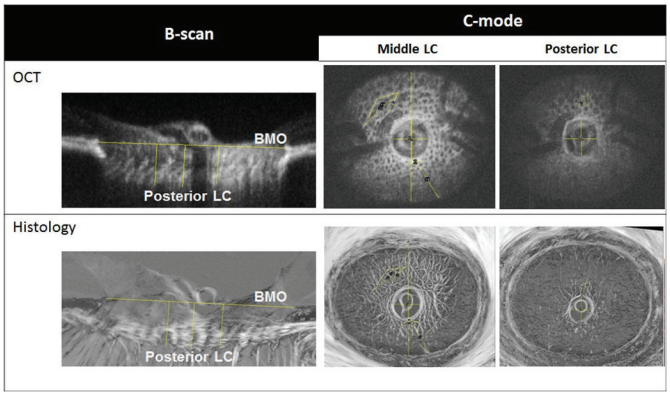

Figure: Comparison of penetration depth and LC microstructure between OCT (top row) and histology (bottom row). Yellow lines illustrate corresponding structures.

	Monkey 1			Monkey 2		
	Scan 1	Scan 2	Scan 3	Scan 1	Scan 2	Scan 3
Posterior LC/Canal						
BMO Area (10^2 μm²)	968	961	939	825	829	830
Posterior Lamina Area (10^2 μm²)	454	488	494	463	491	495
Posterior Lamina/BMO (%)	**46.9**	**50.7**	**52.5**	**55.9**	**59.1**	**59.6**

Table: Results of delineating posterior LC in the OCT scans.

Commercial Relationships: HUONG TRAN, None; **Bo Wang**, None; **Ning-Jiun Jan**, None; **Gadi Wollstein**, None; **Matthew A. Smith**, None; **Larry Kagemann**, None; **Hiroshi Ishikawa**, None; **Joel S. Schuman**, Carl Zeiss Meditec (P); **Elizabeth Tyler-Kabara**, None; **Ian A. Sigal**, None
Support: NIH CORE Grant P30 EY008098; Eye and Ear Foundation of Pittsburgh, PA; Unrestricted Grant from Research to Prevent Blindness,New York,NY

Program Number: 914 **Poster Board Number:** A0266
Presentation Time: 3:15 PM–5:00 PM

A Comparison of Measuring Methods for Anterior Lamina Cribrosa Surface Depth

Je Hyun Seo[1], Tae-Woo Kim[2], Robert N. Weinreb[3]. [1]Department of Ophthalmology, Pusan Nat, Yangsan, Republic of Korea; [2]Ophthalmology, Seoul National University College of Medicine, Seoul National University Bundang Hospital, Seongnam, Republic of Korea; [3]Hamilton Glaucoma Center and Department of Ophthalmology, University of California San Diego, La Jolla, CA.

Purpose: To compare the measuring methods for the anterior lamina cribrosa surface (ALCS) depths in healthy and glaucomatous eyes using enhanced depth imaging (EDI) spectral domain-optical coherence tomography (SD-OCT).
Methods: A total of seventy eyes from 30 normal subjects and 40 glaucoma patients were enrolled. Serial horizontal B-scans of the optic nerve head were obtained using EDI SD-OCT. ALCS depths (perpendicular distance from the Bruch's membrane opening plane to the ALCS) were measured at 3 B-scans from 3 locations (superior-midperiphery, mid-horizontal, and inferior-midperiphery) in each eye by two methods. In Method A, the ALCS depth in each B-scan was defined as the average of the 3 measurements from 3 points (the maximum depth point and two additional points, temporally 100 μm, 200 μm apart from the maximum depth point). In Method B, a smooth contour line was drawn following the ALCS and the maximum depth was considered as the ALCS depth in each B-scan. Intraclass correlation coefficient (ICC) was calculated to determine the interobserver agreement of each method. Bland-Altman Plot was performed to determine the agreement of the ACLC values measured by Method A and B. A regression analysis was performed to identify the relationship between clinical parameters and the ALCS depth measured by Method A and B.
Results: The interobserver ICCs for Method A and B were 0.964-0.980 and 0.976-0.988, respectively. Bland-Altman plot showed a tendency that ALCS depth measured by Method B is increasingly greater than that measured by Method A in eyes with larger ALCS depth. ALCS depths measured by Method A and B were significantly larger in glaucomatous eyes than in healthy eyes (567.76 ± 140.48 vs. 411.53 ± 89.51, $P < 0.0001$ and 590.04 ± 146.83 vs. 416.73 ± 99.35, $P < 0.0001$, respectively). A higher baseline IOP was significantly correlated with ALCS depth measured by both Method A (partial correlation coefficient = 0.640, $P = 0.001$) and by method B (partial correlation coefficient = 0.619, $P = 0.001$).
Conclusions: This study compared the two different measuring methods of ALCS depth. Both methods had low measurement variability and showed the difference between the healthy subjects and glaucoma patients. ALCS depths measured by both methods were correlated with baseline IOP in glaucoma patients.

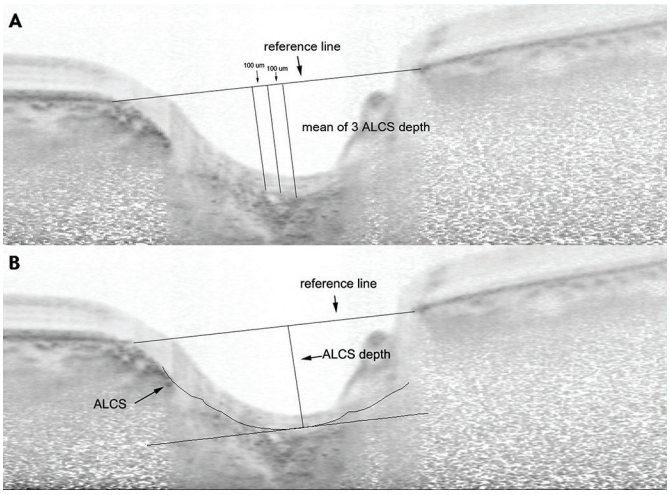

Measurement of ALCS Depth. (A) Method A. (B) Method B

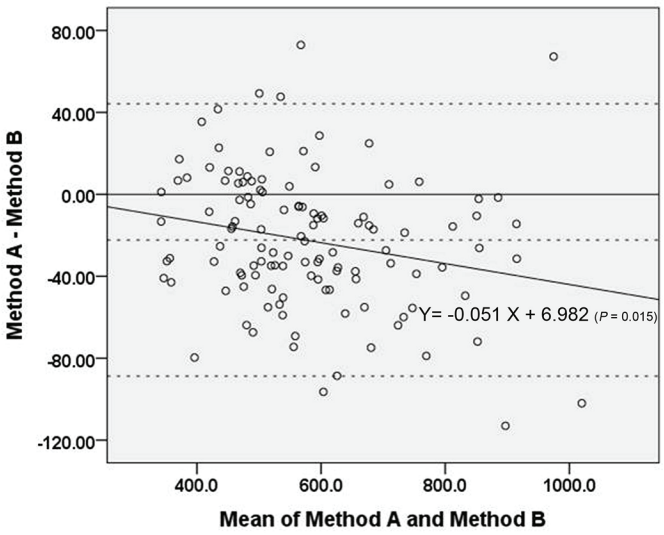

Bland-Altman Plot of ALCS depth of enrolled patients.

Commercial Relationships: Je Hyun Seo, None; **Tae-Woo Kim**, None; **Robert N. Weinreb**, Heidelberg Engineering (C)
Support: Supported by National Research Foundation of Korea Grant funded by Korean Government 2013R1A1A1A05004781

Program Number: 915 **Poster Board Number:** A0267
Presentation Time: 3:15 PM–5:00 PM
Stereoscopic infrared imaging of the optic nerve in glaucoma

Vivek P. Vasuki, Puneet S. Braich, Dane Stewart, Vikram Brar. Ophthalmology, VCU, Richmond, VA.

Purpose: Evaluation of cup to disc ratios has not been explored using infrared technology, although it is widely known that infrared light penetrates deeper into the eye than conventional imaging modalities. We aim to evaluate whether stereoscopic infrared (SIR) photography provides an enhanced assessment of the cup to disc ratio compared to stereoscopic color (SC) and red-free (SRF) images.
Methods: Seventeen eyes diagnosed with glaucoma or as glaucoma suspects were evaluated. Eyes with concurrent vitreoretinal disease or significant media opacities were excluded. All eyes received SIR, SC, and SRF photos in addition to spectral domain OCT imaging. All data was de-identified and presented randomly before being analyzed to avoid bias by sequential comparison of the same eye. Horizontal and vertical cup to disc ratios were measured by a single ophthalmologist. A pairwise comparison was made between all 3 groups with a stringent Bonferroni correction of the p-value (i.e. p was not 0.05, but 0.0167).
Results: The mean of the differences in vertical cup to disc ratios were 0.07 (SC vs. SRF, $p < 0.01$), 0.11 (SC vs. SIR, $p<0.01$) and 0.04 (SIR vs. SRF, $p =0.08$). The mean differences in horizontal cup to disc ratios were 0.11 (SC vs. SRF, $p < 0.01$), 0.11 (SC vs. SIR, $p<0.01$) and 0.006 (SIR vs. SRF, $p =0.81$). When SC photos revealed a vertical cup to disc ratio of less than 0.45, neither of the other modalities deviated by more than 0.1 of that assessment. However, when vertical cup to disc ratios were larger than 0.5 on SC photos, 40% of the time SRF photos were able to find an additional difference of 0.15 ($p<0.01$). SIR was able to detect a 0.15 additional difference 50% of the time ($p<0.01$). When horizontal cup to disc ratios were larger than 0.5 on SC photos, 24% of the time SRF and SIR photos were able to find an additional difference of 0.15 ($p<0.01$). The range of differences measured between techniques was 0-0.3. The greatest difference in examiner estimation was noted in eyes with cup to disc ratios larger than 0.5.
Conclusions: Our results suggest that a larger estimation of horizontal and vertical cup to disc ratios is possible with stereoscopic infrared imaging compared to color stereoscopic photos. This suggests that more of the optic cup is being visualized with infrared imaging, particularly in eyes with ratios higher than 0.5. A larger sample size may indicate that SIR measures larger vertical cup to disc ratios than SRF imaging.

Commercial Relationships: Vivek P. Vasuki, None; **Puneet S. Braich**, None; **Dane Stewart**, None; **Vikram Brar**, None

Program Number: 916 **Poster Board Number:** A0268
Presentation Time: 3:15 PM–5:00 PM
Does optic nerve head(ONH) remodeling precedes retinal nerve fiber layer(RNFL) thinning in glaucoma patients?

Guihua Xu, Christopher K. Leung. Division of Ophthalmology&Visual Science, The Chinese University of HongKong, HongKong, China.

Purpose: Glaucoma is characterized by progressive loss of retinal ganglion cells and remodeling of the ONH. Animal studies show that optic disc surface height change measured by CSLO precedes RNFL thinning measured by OCT in experimental glaucoma. However, long-term clinical data corroborating this observation is lacking. In this prospective study, we followed 146 eyes of 90 glaucoma patients followed for at least 4 years to determine the sequence of ONH and RNFL changes.
Methods: Eyes were imaged by CSLO (HRT) and SD-OCT (Cirrus HD-OCT) at 4-month intervals for measurement of ONH surface topology and RNFL thickness, respectively. Only images meeting the quality criteria (signal strength ≥8 for OCT; SD≤30μm for HRT) in the same visits were included for analysis. RNFL progression was defined when there were more than 20 pixels coded in red in the RNFL thickness change map analyzed by the Guided Progression Analysis(i.e. consecutive thickness changes greater than the test-retest variability). ONH progression was analyzed with reference to Topographic Change Analysis based on two criteria (less conservative: total clusters inside ONH ≥0.1% of the disc area with a mean depth change of ≥20μm; more conservative: total clusters inside ONH ≥2% of disc area with ≥100μm mean depth change).
Results: The mean follow-up duration was 64.5 months (range: 48.3–76.6 months). FIG 1 shows the Venn diagrams of progression detection using different criteria. 26 and 10 eyes had progression evident in both CSLO and OCT at the final visit, with 17 (65.4%) and 7 eyes (70%) had optic disc surface height depression before RNFL thinning, using the less and more conservative criteria, respectively. Only 6 (23.1%) and 2 (20%) eyes had RNFL thinning detected before ONH surface depression. The agreement between OCT and CSLO progression was poor in both criteria (kappa: 0.074-0.096).
Conclusions: ONH surface depression occurred prior to RNFL thinning in most glaucoma patients. ONH remodeling may be an early sign for therapeutic intervention before irreversible loss of neuronal tissues in glaucoma.

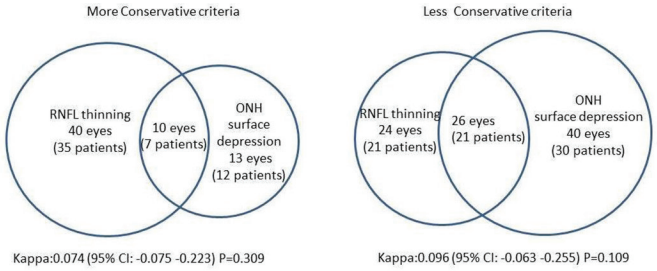

Fig 1 Venn diagrams showing the number of eyes and patients with progression detected by OCT and CSLO using the less and more conservative criteria.

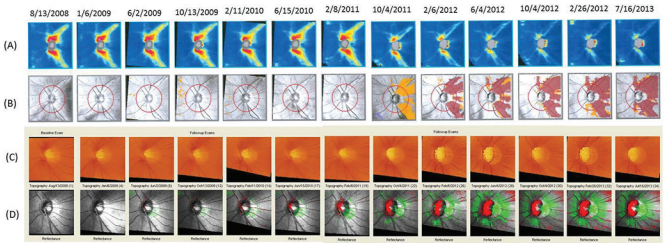

Fig 2 Serial RNFL thickness maps (A), RNFL thickness change maps (B), ONH surface topology maps (C), ONH significance maps (D) of a glaucomatous eye followed for 59.4 months.

Commercial Relationships: Guihua Xu, None; **Christopher K. Leung**, Carl Zeiss Meditec (F)

Program Number: 917 **Poster Board Number:** A0269
Presentation Time: 3:15 PM–5:00 PM
Computer-Aided Diagnosis: Screening for Glaucomatous Defect on Red-Free Fundus Photography using Polarimetric Techniques
Jinho Lee[1], Jee-Yong Lee[2], Ki Ho Park[1], Jong Hyo Kim[2]. [1]Department of Ophthalmology, Seoul National University Hospital, Seoul, Republic of Korea; [2]Graduate School of Convergence Science and Technology, Seoul National University, Seoul, Republic of Korea.
Purpose: To develop a computer program that determines whether there is a retinal nerve fiber layer (RNFL) defect in a given fundus image and, if there is, where it presents.
Methods: The given red-free fundus image was converted to non-extorted image (the optic disc center was at the level of the macula). The intensity profile was normalized to enhance the contrast. The region of interest (ROI) was set as the circumferential area surrounding the optic disc (internal diameter: 2 disc diameters [DD], external diameter: 3 DD). The temporal half of the ROI was converted to a polarimetric image. After removing the blood vessels with a Frangi filter, the differential gradients were calculated along the angular axis. The average curvature was calculated sector-by-sector based on the gradient data, and the local maximum value was obtained. If the maximum value was greater than the cut-off value, the sector was considered to be an RNFL defect.
The images of 100 normal healthy controls and 100 open-angle glaucoma patients were enrolled as age- and sex-matched samples. When both of a subject's eyes were eligible, the image of one eye was randomly selected. Maximum curvatures of two groups were compared and an ROC analysis was performed to determine the reliability of this system and to set the optimum cut-off value, as the minimum acceptable sensitivity was set to 70.0%.
Results: The mean ages of the control group and glaucoma group subjects were 57.5 ± 12.8 and 58.7 ± 11.2 years, respectively (p=0.456). In the control group, fifty-two of the 100 subjects were male, while in the glaucoma group, 45 of 100 were male (p=0.322). In the glaucoma group, the mean deviation was -4.90 ± 5.40 dB. There was a significant difference of maximum curvature between the two groups (14.37 ± 5.13 in control, 20.67 ± 10.56 in glaucoma group, p<0.001). In the ROC analysis, the area under curve (AUC) was 0.711. The probability of asymptomatic significance (less than 0.001) and the asymptomatic confidence interval (95% CI; 0.639 - 0.782) suggested that the maximum curvature is highly associated with RNFL defect. Considering a minimum acceptable sensitivity of 70.0%, the specificity, for a cut-off value of 14.84 was determined to be 62.0%.
Conclusions: The proposed computer program could be an effective screening and early-detection tool for physicians.
Commercial Relationships: Jinho Lee, None; **Jee-Yong Lee**, None; **Ki Ho Park**, None; **Jong Hyo Kim**, None

Program Number: 918 **Poster Board Number:** A0270
Presentation Time: 3:15 PM–5:00 PM
Choroidal Vessel Cross-Sectional Area Before and After Trabeculectomy
Angelique Pillar, Osamah Saeedi. Ophthalmology, University of Maryland, Baltimore, MD.
Purpose: We have previously shown that choroidal thickness has an inverse linear relationship with intraocular pressure (IOP) after trabeculectomy. As current methods to isolate choroidal vessels rely on complex algorithms and customized software, our purpose was to develop a simple method of identifying choroidal vessels in ImageJ to understand the relationship between large choroidal vessel area and IOP after trabeculectomy.
Methods: 21 eyes of 20 patients undergoing trabeculectomy were studied in this case series. Patients were examined pre-operatively, then post-operatively at 1 week and 1, 3, and 6 months with IOP checks and Enhanced Depth Imaging SD-OCT (Spectralis, Heidelberg Instruments) centered on the posterior 6 mm surrounding the fovea. Using ImageJ software (NIH Bethesda), the choroid was manually outlined extending from the retinal pigment epithelium to the choroidal-scleral interface. The image was contrast enhanced with histogram equalization and compared to a color gradient-map to determine the extent of the choroidal vessels. A threshold value was set, above which the large choroidal vessels were outlined. The outlined vessel area was then averaged over the 6 mm choroid to obtain choroidal vessel thickness. Interstitial thickness outside of the major vessels was calculated by subtracting the choroidal vessel thickness from the choroidal thickness. The relationship between the change in vascular thickness and change in IOP after trabeculectomy was analyzed using univariate regression analysis and a linear regression model to calculate the coefficient of determination (R2).
Results: 58 OCT image in 16 patients were deemed sufficient for analysis. The average large vessel thickness was 96+/-56 μm and the average choroidal thickness was 220+/-73 μm. The change in vessel thickness statistically significantly correlated with change in IOP after trabeculectomy at one month (P < 0.01). Conversely, change in interstitial thickness was not correlated with change in IOP (P = 0.053). Neither the change in vessel thickness (slope -2.190, R2 0.397) nor the interstitial thickness (slope -1.35, R2 0.241) respected a linear relationship with IOP.
Conclusions: Our data suggest that choroidal vessel cross-sectional area increases with IOP lowering after trabeculectomy, but this relationship is not linear. Furthermore, using our method, interstitial cross-sectional area does not change with IOP lowering trabeculectomy surgery.

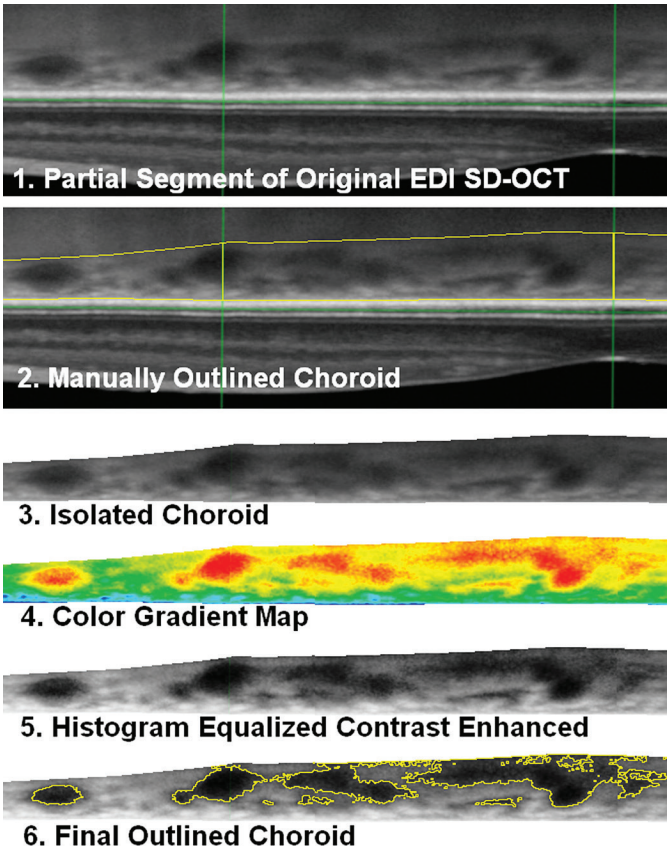

Commercial Relationships: Angelique Pillar, None; **Osamah Saeedi**, None

Program Number: 919 **Poster Board Number:** A0271
Presentation Time: 3:15 PM–5:00 PM
Evaluation of the choroidal thickness in children with primary congenital glaucoma
Mariana Cardoso, Rita Anjos, luisa vieira, Arnaldo D. Santos, Barbara Borges, Luís Pinto, Cristina Ferreira, Ana Xavier, Cristina Brito. Centro Hospitalar Lisboa Central, Porto, Portugal.
Purpose: To evaluate the choroidal thickness (CT) in children with primary congenital glaucoma (PCG) and healthy children.
Methods: Prospective study of children with PCG (glaucoma group) and healthy children. With resource of optical coherence tomography the following measures were made: retinal thickness (RT) and CT at the fovea, 1,5 mm nasal and 1,5 mm temporal to the fovea; peripapillary retinal nerve fiber layer thickness (RNFL) and CT.
Results: Data from 12 eyes of 9 children with PCG and 17 eyes of 9 healthy children were analyzed. Macular CT and RT and peripapillary CT were similar in both groups (p>0,05). However, when patients with high ametropias were excluded, foveal CT was higher in the glaucoma group (p< 0.05). There was a correlation between foveal CT and global RNFL in the glaucoma group (r=0,764; p=0,01) and in the control group (r=0,570; p=0,042).
Conclusions: Although numerous studies have been recently published on the choroidal changes in adult glaucoma, the subject is still controversial. In our study there were no differences between CT in children with or without PCG.
Commercial Relationships: Mariana Cardoso, None; **Rita Anjos**, None; **luisa vieira**, None; **Arnaldo D. Santos**, None; **Barbara Borges**, None; **Luís Pinto**, None; **Cristina Ferreira**, None; **Ana Xavier**, None; **Cristina Brito**, None

Program Number: 920 **Poster Board Number:** A0272
Presentation Time: 3:15 PM–5:00 PM
Anterior Segment Enhanced-Depth Imaging Optical Coherence Tomography for Imaging the Lamina Cribrosa Ex Vivo
Sung Chul Park[1, 2], Tatyana Milman[3], Pooja Mahadeshwar[1], Jason L. Chien[1], Jeffrey M. Liebmann[1, 4], Robert Ritch[1, 2]. [1]Moise and Chella Safra Advanced Ocular Imaging Laboratory, Einhorn Clinical Research Center, New York Eye and Ear Infirmary of the Mount Sinai Health System, New York, NY; [2]Department of Ophthalmology, New York Medical College, Valhalla, NY; [3]Department of Pathology, New York Eye and Ear Infirmary of the Mount Sinai Health System, New York, NY; [4]Department of Ophthalmology, New York University School of Medicine, New York, NY.
Purpose: To investigate the use of anterior segment enhanced-depth imaging optical coherence tomography (EDI OCT) in imaging the lamina cribrosa (LC) of ex vivo eyes.
Methods: After removing the anterior segment and the vitreous from fresh enucleated pig eyes, posterior segment tissue containing the optic nerve head and peripapillary sclera (Fig A) was placed on a custom-designed eye holder (Fig 1B). To stabilize the eye holder on the OCT device, an eye holder frame was used (Fig 1C). Serial horizontal (15°x10°) and vertical (10°x15°) EDI OCT B-scans (distance between scans: ~32 μm) of the optic nerve head were obtained from the prepared tissue using the anterior segment module of spectral-domain OCT (Spectralis; Heidelberg Engineering GmbH, Heidelberg, Germany). Different conditions were tested to obtain better-quality OCT images of the LC. After EDI OCT, serial horizontal or vertical histological sections were obtained (distance between sections: ~5 μm), stained (Periodic Acid-Schiff) and photographed. Structures identified in the histological sections were compared with structures in the matched EDI OCT B-scans. 3-dimensional images of the LC were reconstructed using serial EDI OCT B-scans after manually delineating the LC beams.
Results: Optic nerve heads of 3 enucleated pig eyes were imaged using EDI OCT and then examined histologically. The LC was more clearly visualized when the retina and part of prelaminar tissue were removed (Fig 1D, 1E) and when the tissue surface was kept moist during EDI OCT (Fig 1F, 1G). The LC image quality was similar between pre-fixation and post-fixation tissues (Fig 1H, 1I). The LC was also visualized successfully using the OCT's posterior segment module when a +20-diopter lens was placed between the tissue and OCT using a custom-designed lens holder, to substitute for the refractive power of the anterior portion of the eyeball (Fig 1J, 1K). EDI OCT B-scans accurately matched serial histological sections and identified the LC beams and its continuity with the retrolaminar glial columns (Fig 2A-2F). 3-dimensional images of the LC were successfully reconstructed using EDI OCT B-scans (Fig 2G, 2H).
Conclusions: High-resolution cross-sectional images can be obtained using anterior segment EDI OCT when the retina and part of prelaminar tissue are removed. Anterior segment EDI OCT may be useful in evaluating the LC in ex vivo eyes for glaucoma research.

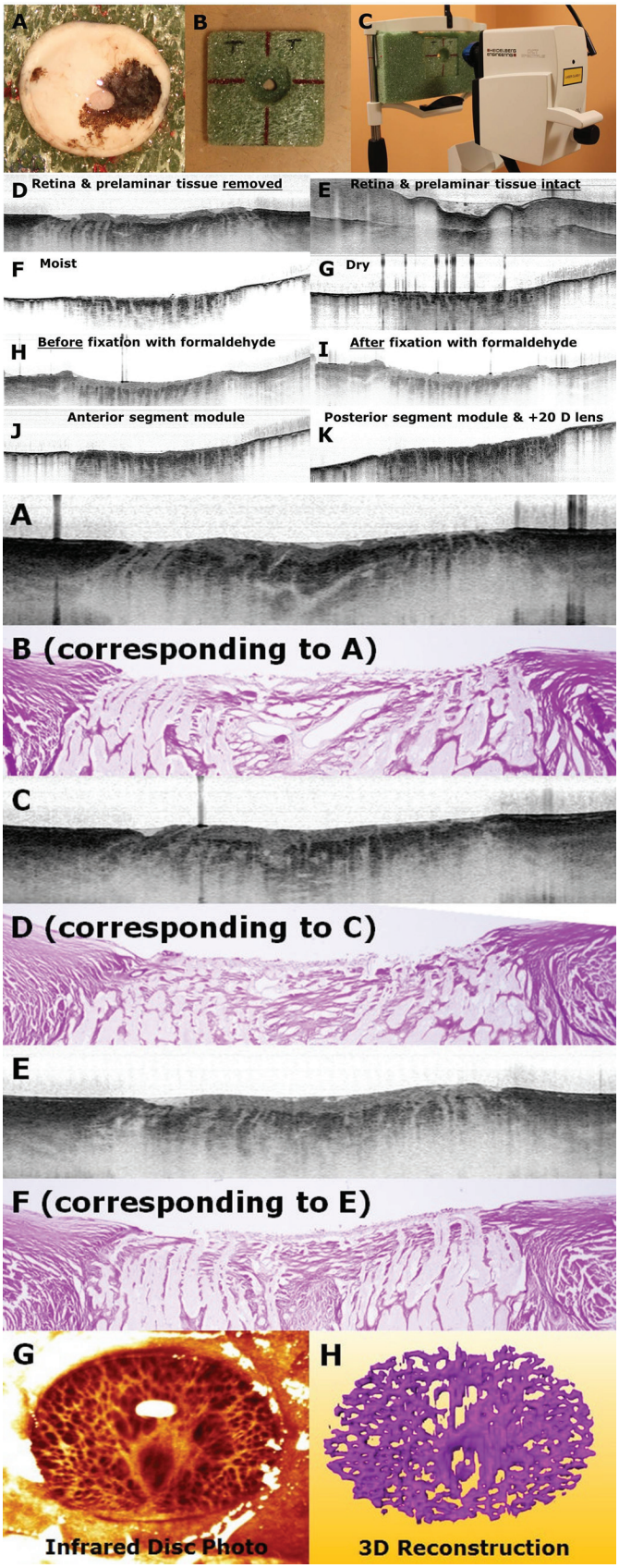

Commercial Relationships: Sung Chul Park, Heidelberg Engineering, GmbH (F), Heidelberg Engineering, GmbH (R); **Tatyana Milman**, None; **Pooja Mahadeshwar**, None; **Jason L. Chien**, None; **Jeffrey M. Liebmann**, Carl Zeiss Meditech, Inc. (F), Heidelberg Engineering, GmbH (C), Heidelberg Engineering, GmbH (F), Optovue, inc (F), Topcon, Inc (F); **Robert Ritch**, None
Support: HRH Prince Ahmed bin Abdulaziz Al-Saud Research Fund of the New York Glaucoma Research Institute, American Glaucoma Society MAPS Award, Peter Crowley Research Fund of the New York Eye and Ear Infirmary

Program Number: 921 **Poster Board Number:** A0273
Presentation Time: 3:15 PM–5:00 PM

STAPHYLOMA SHAPE IN MYOPIC EYES WITH OR WITHOUT GLAUCOMA

Tomoko Asai, Yasushi Ikuno, Atsuya Miki, Shinichi Usui, Kohji Nishida. Ophthalmology, Osaka Univ Grad Sch of Med, Suita, Japan.

Purpose: Recently, myopia was found to increase the susceptibility to intraocular pressure and myopic eyes were at higher risk of developing open-angle glaucoma (OAG). The pathogenesis has been postulated to be morphologic changes around the optic nerve head (ONH) along with axial length elongation. We recently found that the peripapillary morphology is related closely to the type of posterior staphyloma (PS). We compared the PS shape with and without OAG using swept-source optical coherence tomography (SS-OCT).
Methods: We retrospectively studied highly myopic eyes (refractive error <-6 diopters [D] or axial length >26 mm) with (group G, 74 eyes) and without (group N, 83 eyes) glaucomatous optic neuropathy. Only eyes with OAG were included. The depth of the posterior staphyloma was measured in a 12-mm horizontal SS-OCT scan. The staphyloma depth was defined as the average distance between the position of the retinal pigment epithelium (RPE) under the fovea and that 3 mm temporal or nasal to the fovea. The shape of the PS was evaluated by the relative location of the fovea and the ONH. The optic disc type was one in which the foveal surface was more anterior than the anterior surface of the pre-laminar tissue and vice versa for the non-optic disc type (Fig.).
Results: The mean refractive error was -8.42 ± 0.72 D in group G and -11.04 ± 0.58 D in group N (P=0.04). The mean axial length was 29.94 ± 0.19 mm in group G and 28.70 ± 0.18 mm in group N (P<0.01). The staphyloma was significantly deeper in group N (335.0 ± 22.6 μm) compared with group G (192.1 ± 24.4 μm) (P=0.04). The incidence of the optic disc type in group G was significantly higher than that in group N (P=0.04). In group G, there was no significant correlation between the mean deviation value in Humphrey visual field test and the staphyloma depth (P=0.58) or staphyloma shape (P=0.46).
Conclusions: Eyes with OAG have specific characteristics in myopic eyes. The morphologic changes seen in these eyes seem to be related to the increased risk.

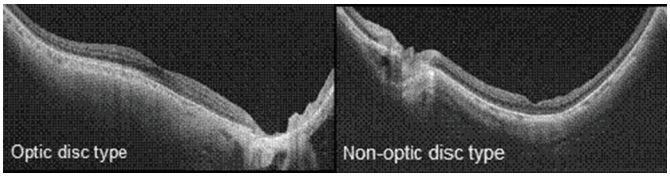

Commercial Relationships: Tomoko Asai, None; **Yasushi Ikuno**, None; **Atsuya Miki**, Nidek (C); **Shinichi Usui**, None; **Kohji Nishida**, None

Program Number: 922 **Poster Board Number:** A0274
Presentation Time: 3:15 PM–5:00 PM
Inter-eye Differences in Bilaterally Myopic Patients with Unilateral Normal-tension Glaucoma
Won Hyuk Oh[1], Young Tae Kong[2], Seok Hwan Kim[3]. [1]Ophthalmology, Sanggye Paik Hospital, Seoul, Republic of Korea; [2]Kong Eye Clinic, Seoul, Republic of Korea; [3]Ophthalmology, Seoul National University Boramae Hospital, Seoul, Republic of Korea.
Purpose: To evaluate the inter-eye differences in bilaterally myopic patients with unilateral normal-tension glaucoma (NTG).
Methods: Bilaterally myopic patients with unilateral NTG were consecutively enrolled. Both eyes of each individual were compared with regard to intraocular pressure (IOP), spectral-domain optical coherence tomography parameters (circumpapillary retinal nerve fiber layer [cpRNFL] thickness, disc area, and β-zone parapapillary atrophy [PPA] area), refractive error, and axial length (AL).
Results: Thirty-six bilaterally myopic patients with unilateral NTG were included. The untreated mean and highest IOP of NTG eyes were not significantly different from those of contralateral non-glaucomatous eyes (p = 0.837; p = 0.908, respectively). Average, superior and inferior quadrants of cpRNFL thickness in NTG eyes were thinner than those obtained for contralateral non-glaucomatous eyes (p = 0.000; p = 0.000; p = 0.000, respectively). Compared with contralateral non-glaucomatous eyes, NTG eyes exhibited reduced disc areas (1.91 ± 0.54 vs. 2.02 ± 0.50 mm2, p = 0.040), but the β-zone PPA areas in NTG eyes were larger (1.40 ± 0.75 vs. 0.98 ± 0.56 mm2, p = 0.000). NTG eyes had more myopic refractive error and longer AL than contralateral non-glaucomatous eyes (-5.73 ± 1.87 vs. -4.92 ± 2.01 D, p = 0.000; 26.42 ± 1.04 vs. 26.08 ± 1.11 mm, p = 0.000).
Conclusions: In myopic individuals, NTG eyes had longer AL, more myopic refractive error and larger β-zone PPA areas than contralateral non-glaucomatous eyes. Inter-eye AL differences may contribute to the development of NTG in myopes.
Commercial Relationships: Won Hyuk Oh, None; **Young Tae Kong**, None; **Seok Hwan Kim**, None

Program Number: 923 **Poster Board Number:** A0275
Presentation Time: 3:15 PM–5:00 PM
Factors Associated with Anterior Chamber Volume and Iris Volume in Pigment Dispersion Syndrome
Ruojin Ren[1], Christopher C. Teng[1, 2], Sung Chul Park[1, 2], Mugen Liu[1], Lam Lu[1], Gustavo V. De Moraes[1, 3], Jeffrey M. Liebmann[1, 3], Robert Ritch[1, 2]. [1]Moise and Chella Safra Advanced Ocular Imaging Laboratory, Einhorn Clinical Research Center, New York Eye and Ear Infirmary of the Mount Sinai Health System, New York, NY; [2]Department of Ophthalmology, New York Medical College, Valhalla, NY; [3]Department of Ophthalmology, New York University School of Medicine, New York, NY.
Purpose: To investigate clinical factors associated with anterior chamber volume (ACV) and iris volume (IV) in eyes with pigment dispersion syndrome (PDS) with and without ocular hypertension or glaucoma (PG) using swept-source optical coherence tomography (SS-OCT).
Methods: In this cross-sectional study, each participant underwent SS-OCT (Casia SS-1000 OCT; Tomey, Inc., Nagoya, Japan) to obtain 128 volumetric high-resolution radial B-scans centered on the pupil center and a complete ophthalmologic examination including standard automated perimetry (SAP) and spectral-domain OCT retinal nerve fiber layer thickness (RNFLT). Trace lines of the anterior chamber and iris contour were reviewed by a glaucoma specialist and corrected if necessary. ACV and IV were analyzed using the SS-OCT's built-in software. ACV and IV were correlated with the following demographic and clinical factors using a multivariate model: age, phakic refractive error, untreated intraocular pressure (IOP), central cornea thickness (CCT), SAP mean deviation (MD) and RNFLT.
Results: 20 eyes (10 patients; 4 women; mean age, 43±12 years), including 7 PDS eyes and 13 PG eyes, were included. Mean refractive error, central corneal thickness, and SAP mean deviation were -2.56±2.34D, 556.8±27.3μm, and -2.44±3.24dB, respectively (Table 1). Mean ACV was 239±29 mm3 (range, 194–297) and mean iris volume was 44±5 mm3 (range, 37 –54). Greater ACV was associated with higher IOP (p=0.03) and associated with worse SAP MD (p=0.04) and lower CCT (p=0.04). IV was not related to these factors (all p>0.05).
Conclusions: Greater ACV appears to be greater with higher IOP and worse visual field status in PDS and PG eyes. Greater ACV may be related to more frequent or wider iridozonular contact and enhanced pigment liberation.

Table 1. Characteristics of the 10 participants and the 20 eyes in the study.

	Mean ± Standard Deviation	Range
Age (years)	43.0±12.0	26.0 – 59.0
Refractive Error (D)	-2.56±2.34	-6.50 – 3.75
Intraocular Pressure (mmHg)	21.7±8.7	12.0 – 48.0
Central Corneal Thickness (μm)	556.8±27.3	509.0 – 598.0
Mean Deviation (dB)	-2.44±3.24	-10.92 – 1.36
SDOCT RNFL Thickness (μm)	81.73±17.62	57 – 118
Anterior Chamber Volume (mm^3)	239.45±28.91	193.80– 297.15
Iris Volume (mm^3)	44.43±4.66	37.23 – 54.39

Commercial Relationships: Ruojin Ren, None; **Christopher C. Teng**, None; **Sung Chul Park**, None; **Mugen Liu**, None; **Lam Lu**, None; **Gustavo V. De Moraes**, None; **Jeffrey M. Liebmann**, Allergan, Inc. (C), Bausch & Lomb, Inc. (C), Carl Zeiss Meditech, Inc. (F), Diopysis, inc. (C), Heidelberg Engineering, GmbH (C), Heidelberg Engineering, GmbH (F), Merz Phamaceuticals, Inc. (C), National Institute of Health (F), National Institutes of Health (F), New York Glaucoma Research Institute (F), New York Glaucoma Research Institute Alcon, Inc (C), Optovue, inc. (F), Quark Pharmaceuticals, Inc. (F), Reichert, Inc. (F), Sensimed, Inc. (F), Topcon, Inc. (F), Valeant Pharmaceutiicals, Inc. (C); **Robert Ritch**, None
Support: 'Gildor Research Fund of the New York Glaucoma Research Institute', 'James Cox Chambers Research Fund of the New York Eye and Ear Infirmary' and 'Peter Crowley Research Fund of the New York Eye and Ear Infirmary'

Program Number: 924 **Poster Board Number:** A0276
Presentation Time: 3:15 PM–5:00 PM
Agreement between gonioscopy and ultrasound biomicroscopy in the assessment of the anterior chamber angle, before and after laser peripheral iridotomy
Claudia Cortes Alcocer[1], Mariana Mayorquin-Ruiz[2], Jesus Jimenez-Roman[1]. [1]Glaucoma, APEC, Mexico City, Mexico; [2]Ultrasound, APEC, Mexico City, Mexico.
Purpose: To assess the agreement between gonioscopy and ultrasound biomicroscopy (UBM) in the diagnosis of eyes with narrow angles. To evaluate the iridocorneal angle widening following laser peripheral iridotomy (LPI).
Methods: This is a prospective, longitudinal and comparative cohort study. We included patients with clinical diagnosis of narrow angle who were scheduled to laser peripheral iridectomy . All patients underwent a complete ophthalmologic examination including best corrected visual acuity (BCVA) assessment with protocol Snellen chart refraction, gonioscopic examination (Shaffer Scale), Intraocular pressure measurement with Goldman applanation tonometer.

The UBM was performed before the LPI and 1 week before the procedure.
We measured the angle opening distance at 500 μm from the scleral spur (AOD500) the iridotrabecular angle (TIA) and the trabecular to ciliar process distance (TCPD). Each quadrant of the anterior chamber angle was taken as an independent observational unit. Results were analyzed using the Wilcoxon signed-rank test and a T-student for related samples.
Results: We enrolled 22 eyes (11 patients) with narrow angle. The mean age was 60.8 ± 5.3 years, 9 were female 2 men. The mean intraocular pressure was 13.8 mmHg and the BCVA was 20/30. The mean gonioscopy grade increased significantly from 1.95 to 3.00 (Po 0.001) . The angles widened 6.34 ° from 13.49° pre iridectomy to 19.83° post iridectomy. And so the AOD500 and the TCPD change from 165.93 μm to 254.77 μm and 766.91 μm to 787.72 μm respectively. The laser used was Nd:YAG the mean power used was 6.3 mJ and the treated quadrant were 23 % inferior and 77% superior in which is observed the mayor widening of the angle.
Conclusions: Changes in the width of the angle after the laser peripheral iridotomy were detected with both, ultrasound biomicroscopy and gonioscopy but those are much better appreciated by UBM. And it help us to measured with better accuracy the changes and to know if they need re-LPI treatment.
Commercial Relationships: Claudia Cortes Alcocer, None; **Mariana Mayorquin-Ruiz**, None; **Jesus Jimenez-Roman**, None

Program Number: 925 **Poster Board Number:** A0277
Presentation Time: 3:15 PM–5:00 PM
Changes in anterior segment morphology of iris bombé before and after laser peripheral iridotomy in patients with uveitic secondary glaucoma
Wakako Ikegawa, Takashi Suzuki, Shiro Mizoue, Yuichi Ohashi.
Ophthalmology, Ehime University School of Medicine, Toon, Japan.
Purpose: Iris bombé and acute pupillary block glaucoma are severe complications of uveitis, and little is known about anterior segment (AS) morphology in angle acute closure of iris bombé. The aim of this work was to quantify changes in AS parameters after laser peripheral iridotomy (LPI) using AS optical coherence tomography (OCT) in iris bombé.
Methods: Seven patients with iris bombé caused by anterior uveitis were enrolled, and AS images were captured at pre-LPI and more than 2weeks after LPI (post-LPI) using AS OCT (Tomey, Casia). Six of Seven patients were imaged before iris bombé. Anterior chamber depth (ACD), anterior chamber volume (ACV), iris volume (IV), iris curvature (IC), iris thickness at 500 μm from the scleral spur (IT-1),in the middle between scleral spar and pupillary margin (IT-2) and 500 μm from pupillary margin (IT-3), and Anterior chamber angle (ACA) parameters [angle opening distance (AOD750) and trabecular iris space area (TISA750)] were analyzed.
Results: Since one patient had bilateral iris bombé, eight eyes in seven patients were investigated. Mean ACD (2.17 vs. 2.52mm), ACV (59.66 vs. 126.46 mm3), ACA parameters (AOD750 [0.10 vs. 0.69 mm] and TISA750 [0.072 vs. 0.33 mm2] at pre-LPI increased at post-LPI (ACD: $P < 0.05$; TISA750: $P<0.01$; ACV and AOD750: $P<0.001$). Mean IT-1 (0.25 vs. 0.37 mm) and IT-2 (0.32 vs. 0.39 mm) but not IT-3 (0.29 vs. 0.27 mm) increased at post-LPI (IT-1: $P<0.01$; IT-2: $P<0.05$; IT-3: $P=0.63$). IC (0.72 vs. 0.18 mm) decreased at post-LPI ($P<0.001$) and IV (27.34 vs. 35.44 mm3) did not changed at post-LPI. Mean IT-1 (0.25 vs. 0.39mm) but not IT-2 (0.32 vs. 0.37mm) and IT-3 (0.29 vs. 0.32mm) were lower than that before iris bombé (IT-1: $P<0.001$; IT-2: $P=0.14$; IT-3: $P=0.34$). There was no significant difference between ACD at pre-LPI and before iris bombé (2.17 vs. 2.37mm, $P=0.20$).
Conclusions: The iris root could be extended and become thinner in iris bombé. LPI in iris bombé could increase ACD, ACV, and ACA parameters.
Commercial Relationships: Wakako Ikegawa, None; **Takashi Suzuki**, None; **Shiro Mizoue**, None; **Yuichi Ohashi**, None

Program Number: 926 **Poster Board Number:** A0278
Presentation Time: 3:15 PM–5:00 PM
Racial differences in trabecular meshwork length with ocular coherence tomography
Diego T. Barbosa, Roland Y. Lee, Rebecca Chen, Shan C. Lin.
Ophthalmology, University of California-San Francisco, San Francisco, CA.
Purpose: Investigate possible differences in trabecular meshwork length among different racial groups.
Methods: We performed ocular coherence tomography (OCT) scans on 326 patients from an ophthalmology clinic at the University of California San Francisco. Only eyes without any previous surgeries were selected. Races included in the study were White, African American, Chinese and Hispanics. Scans were performed with Cirrus OCT from Zeiss using the anterior segment 5 line raster protocol. Patients had to fixate at an external light so that the nasal portion of the eye would be centered for the scan. Scans were done over the limbus area showing the area of the scleral spur. Images were analyzed and trabecular meshwork length was measured from the scleral spur to the endothelium line using imageJ software. We excluded 34 scans due to poor image quality.
Results: Final sample had 292 eyes composed of 37.4% Whites, 13.0% African Americans, 36.6% Chinese and 13.0% Hispanics. The mean trabecular meshwork length was 839μm (SD=129). Range was 531μm to 1325μm. Chinese and Whites had the longest mean trabecular length 860μm (SD=130) and 849μm (SD=126), respectively; Hispanics had 819μm (SD=150) and African Americans had the shortest length of 772 μm (SD=118). After comparing the means using oneway ANOVA with Bonferroni correction, the means for Whites and Chinese were statistically different when compared to African Americans ($p=0.029$ and $p=0.009$). The mean trabecular length value for Hispanics was not statistically different then the other groups.
Conclusions: Our study shows that there is a difference in trabecular meshwork length among racial groups and may provide some insight into the different glaucoma distribution among racial groups.
Commercial Relationships: Diego T. Barbosa, None; **Roland Y. Lee**, None; **Rebecca Chen**, None; **Shan C. Lin**, None
Support: This work was made possible in part, by NIH-NEI EY002162 - Core Grant for Vision Research. This work was made possible in part, by the Research to Prevent Blindness Unrestricted Grant.

Program Number: 927 **Poster Board Number:** A0279
Presentation Time: 3:15 PM–5:00 PM
Visualization of Aqueous Outflow Structures with Spectralis Spectral-Domain Optical Coherence Tomography in the Living Human Eye
Yohko Murakami[1], Siamak Yousefi[2], Amir Marvasti[2], Christopher Bowd[2], Robert N. Weinreb[2], Alex S. Huang[1]. [1]Ophthalmology, University of Southern California, Los Angeles, CA; [2]Hamilton Glaucoma Center, University of California, San Diego, San Diego, CA.
Purpose: To demonstrate noninvasive visualization of aqueous outflow (AO) structures in the living human eye in two (2D) and three (3D) dimensions using the commercially available Spectralis spectral-domain optical coherence tomographer (SD-OCT).

Methods: AO structures, including Schlemm's canal (SC) and collector channels (CC) of both eyes, were imaged by SD-OCT (Spectralis; Heidelberg Engineering) during one setting in a healthy subject. The panning camera head coupled with TruTrack active eye tracking and simultaneous dual-beam imaging allowed for maintained and optimal 360 degree radial orientation of OCT scans during image acquisition. To enhance image quality and diminish noise, frame-averaged mean images were created with the Automatic Real Time (ART; 8) mean function. Twelve volume scans (161 B-scans; 10 x 15 degree scan angle covering a 5.5 x 8.3 mm region at the limbus) using the anterior segment module on high-resolution setting were obtained centered on each clock hour. Axial resolution of each A-scan was 3.9 um with a lateral resolution of 11 um and distance between B-scans of 35 um. In one clock hour, for each 2D slice, the tissue was discriminated from noise, and SC was detected based on intensity distribution (lower intensity values compared to nearby tissue) and location (in the vicinity of intersection of sclera and iris). Then CC and outflow pathways were detected based on intensity distribution. All identified SC, CC, and outflow pathways regions were fused to create 2-D object slices (Matlab; Mathworks). This information was then compiled as a stack with cropping, re-sizing, surface mapping polygonal reconstruction, and 3D manipulation (Imaris; Bitplane).
Results: SC and CC were readily visible on both the 2D (Figure 1; red box = region of interest; blue boxes depict automated detection of SC and CC) and 3D (Figure 2) images. The 3D image also provided visualization of SC discontinuations. CC branching directly from SC could be visualized with downstream Y-shaped aqueous veins noted.
Conclusions: We present visualization of AO structures in the living human eye using the Spectralis and demonstrate the possibility of 3D reconstruction from conventional 2D images.

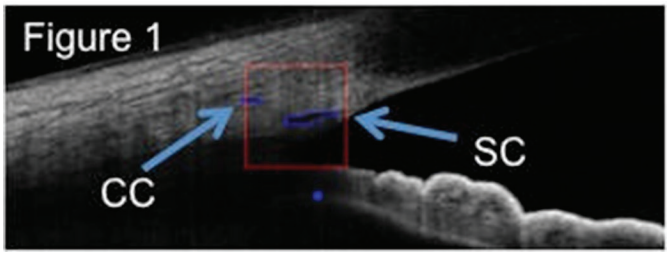

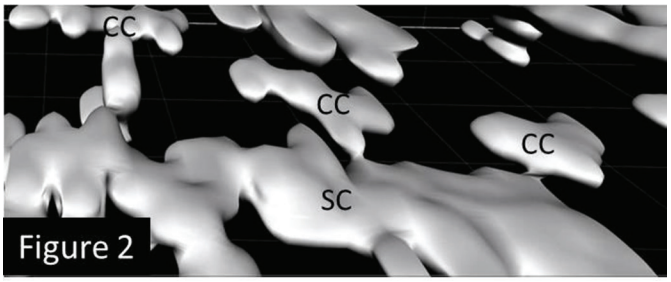

Commercial Relationships: Yohko Murakami, None; **Siamak Yousefi**, None; **Amir Marvasti**, None; **Christopher Bowd**, None; **Robert N. Weinreb**, Aerie (F), Alcon (C), Allergan (C), Bauch & Lomb (C), Carl Zeiss Meditec (C), Carl Zeiss Meditec (F), Genentech (F), Heidelberg Engineering GmbH (F), National Eye Institute (F), Nidek (F), Novartis (F), Optovue (F), Sensimed (C), Topcon (C), Topcon (F); **Alex S. Huang**, None

Program Number: 928 **Poster Board Number:** A0280
Presentation Time: 3:15 PM–5:00 PM
Anterior Segment Imaging-based Subgrouping of Primary Angle Closure Glaucoma
Monisha E. Nongpiur[1, 2], Tianxia Gong[3], Hwee Kuan Lee[3], Michael Loh[3], Shamira Perera[1], Mingguang He[4], Tin Aung[1, 5]. [1]Glaucoma, Singapore Eye Research Institute and Singapore National Eye Centre, Singapore, Singapore; [2]Duke-NUS Graduate Medical School, Singapore, Singapore; [3]Bioinformatics Institute, A*STAR (Agency for Science, Technology and Research), Singapore, Singapore; [4]State Key Laboratory of Ophthalmology, Zhongshan Ophthalmic Center, Sun Yat-sen University, Guangzhou, China; [5]Ophthalmology, Yong Loo Lin School of Medicine, National University of Singapore,, Singapore, Singapore.
Purpose: We recently showed that it was possible to subgroup primary angle closure suspects (PACS) based on anterior segment optical coherence tomography (ASOCT) imaging. The purpose of this study was to identify whether this was also credible for primary angle-closure glaucoma (PACG); and to determine the characteristics of such subgroups.
Methods: We evaluated 210 PACG subjects. All subjects underwent gonioscopy and ASOCT imaging (Carl Zeiss Meditec, Dublin, CA). Customized software (Zhongshan Angle Assessment Program, Guangzhou, China) was used to measure ASOCT parameters. An agglomerative hierarchical clustering method was first used to determine the optimum number of parameters to be included in the determination of subgroups. Then the best number of subgroups was determined using Akaike Information Criterion (AIC) and Gaussian Mixture Model (GMM) methods.
Results: The mean age of the subjects was 68.3 years, and 60.2% were female. After hierarchical clustering, either 1 or 2 parameters from each cluster were chosen to be representative of related parameters. The parameters included were iris area, anterior chamber depth (ACD), anterior chamber width (ACW), and lens vault (LV). The optimal number of subgroups using GMM analysis and AIC was 3. Subgroup 1 (N=89; 42.4%) was characterized by a large iris area, subgroup 2 (N=24; 11.4%) by a large LV and a shallow ACD, whereas subgroup 3 (N=97; 46.2%) displayed only intermediate values across iris area, LV and ACD.
Conclusions: Mirroring our findings for PACS, we also identified three distinct subgroups of PACG subjects based on ASOCT imaging.
Commercial Relationships: Monisha E. Nongpiur, None; **Tianxia Gong**, None; **Hwee Kuan Lee**, None; **Michael Loh**, None; **Shamira Perera**, None; **Mingguang He**, None; **Tin Aung**, None
Support: A*STAR BMRC TCRP Grant

Program Number: 929 **Poster Board Number:** A0281
Presentation Time: 3:15 PM–5:00 PM
Characterizing Angle Landmarks with Anterior Segment Optical Coherence Tomography
Eric L. Crowell[1, 2], Mark E. Gold[1], Alice Chuang[1], Laura Baker[2], Robert M. Feldman[1, 2], Nicholas P. Bell[1, 2], Lauren S. Blieden[1, 2]. [1]Ruiz Department of Ophthalmology and Visual Science, The University of Texas Medical School at Houston, Houston, TX; [2]Robert Cizik Eye Clinic, Houston, TX.
Purpose: Identify the presence/absence of 3 identifiable landmarks: trabecular meshwork (TM), TM interface, and a novel landmark termed Bell's Layer (BL), which is a juxtatrabecular landmark visible on anterior segment optical coherence tomography (ASOCT)
Methods: This is a retrospective review of imaging data from prior IRB-approved studies. Horizontal images from 2D angle analysis scans using a CASIA SS-1000 (Tomey, Nagoya, Japan) were evaluated by a masked, experienced reader for presence/absence of

TM, TM interface, and BL using the ACAI (Houston, TX) software. Only one eye was included per participant. Logistic regression was used to analyze the potential factors of age, gender, race, IOP, gonioscopy grade, angle location and history/presence of surgery on visibility of these structures.

Results: A total of 173 horizontal images were included in this study. The mean age of participants was 52.4 (+15.6) years old with 114 female (66%) and 109 (63%) white. No factors were found to affect the visibility of BL; however, it is more visible in white and black ($p<0.05$) populations than Asians in paired comparison. It is also more likely to be visible in eyes with a gonioscopy grade of E than of A (P=0.047). Being female is 2.86 times (P=0.0069) and a nasal angle is 2.98 times (P=0.0003) more likely to have an invisible TM. Additionally, being female is 1.78 times (P=0.0314) and a nasal angle is 2.22 times (P=0.0021) more likely to have an invisible TM interface.

Conclusions: Gender and location in the angle are 2 factors affecting visibility of TM and TM interface, while BL is more visible in non-Asian populations and eyes with wide open gonioscopy. We have identified a novel ASOCT landmark adjacent to the TM interface (Schlemm's canal) which has not previously been identified or described. Further study is needed to determine the pathophysiologic relevance. We hypothesize that BL may correlate with directionally aligned fibers seen surgically when entering Schlemm's canal via an *ab externo* approach.

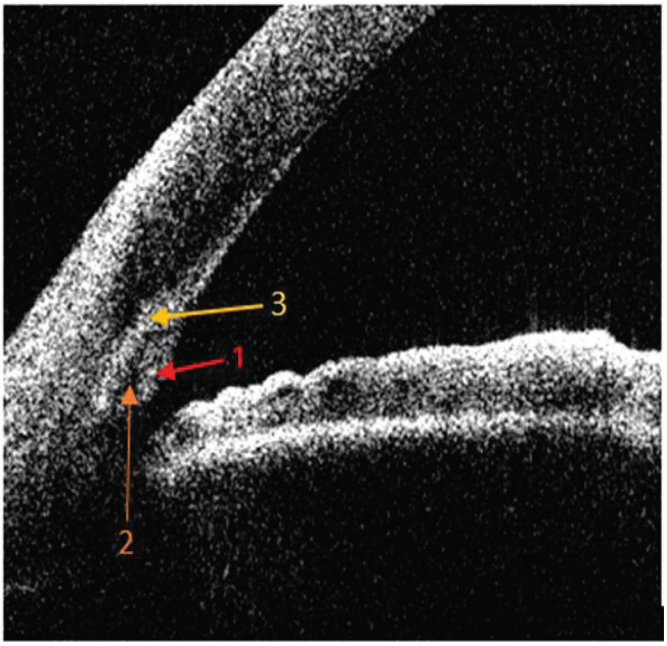

Figure 1: 2D angle image demonstrating landmarks 1) trabecular meshwork (TM), 2) TM interface (Schlemm's canal), and 3) Bell's Layer.

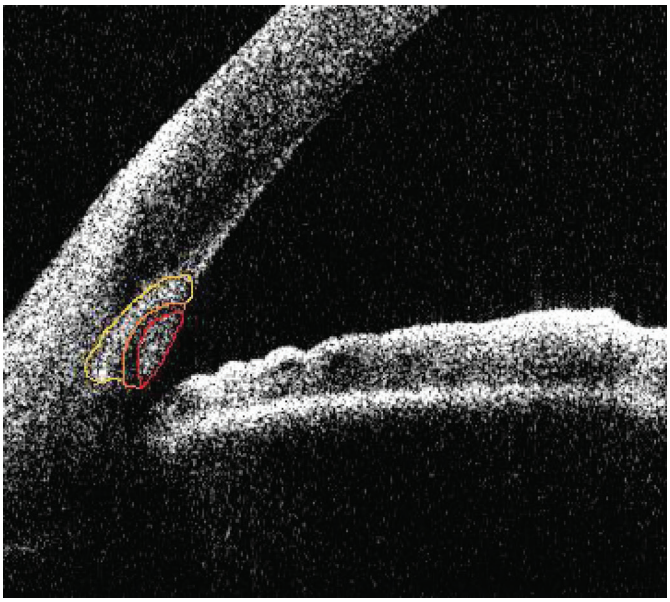

Figure 2: 2D angle image outlining landmarks: trabecular meshwork (TM: red), TM Interface (Schlemm's canal; orange), and Bell's Layer (yellow).

Commercial Relationships: Eric L. Crowell, None; **Mark E. Gold**, None; **Alice Chuang**, None; **Laura Baker**, None; **Robert M. Feldman**, Tomey Corporation (F); **Nicholas P. Bell**, None; **Lauren S. Blieden**, None

Support: NEI Vision Core Grant P30EY010608; Challenge Grant from Research to Prevent Blindness to The University of Texas Medical School at Houston; Hermann Eye Fund

Program Number: 930 **Poster Board Number:** A0282
Presentation Time: 3:15 PM–5:00 PM

Trabecular-Iris Circumference Volume in Normal Open Angle Eyes Using Swept Source Fourier Domain Anterior Segment Optical Coherence Tomography

Mohammed Rigi[1], Donna Nguyen[2], Lauren S. Blieden[1, 3], Nicholas P. Bell[1, 3], Laura Baker[1], Alice Chuang[3], Robert M. Feldman[1, 3]. [1]Robert Cizik Eye Clinic, Houston, TX; [2]Glaucoma Service, South Texas Veterans Health Care System, San Antonio, TX; [3]Ruiz Department of Ophthalmology and Visual Science, The University of Texas Medical School at Houston, Houston, TX.

Purpose: Evaluation of the anterior chamber angle is essential to diagnose and manage eyes with angle closure disease. Monitoring changes in angle configuration after treatment, such as laser peripheral iridotomy (LPI) or lens extraction (LE), depends on the accuracy and precision of angle measurements. Anterior segment optical coherence tomography (ASOCT) has been used to quantitatively measure these parameters. This study uses ASOCT imaging to evaluate the normal range of a new parameter Trabecular-Iris Circumference Volume (TICV). TICV is determined by integrating Trabecular-Iris Space Area (TISA) from 128 scans over 360 degrees in an eye (Figure 1).

Methods: Participants with Spaeth D or E gonioscopic grading and otherwise normal appearing anterior segments were recruited. One eye from each participant was included. 3D ASOCT images were obtained with the CASIA SS-1000 (Tomey, Nagoya, Japan). TISA500 and TICV500 were calculated. Analysis of covariance was performed to examine the effects of spherical equivalent and its interaction with age groups.

Results: Ninety eyes were included. Sixty percent of participants were female, and participants had a mean age of 50.0 ±15.1 years (ranged 20-79). Sixty percent were White, 25.6% Black, 10% Hispanic, and 4.4% Asian. The anterior chamber angle parameters show age-related reduction of anterior angle parameters (P<0.0001; Table 1). Excluding extreme myopia (more than -12D), the data suggests that angle volume increases with increased myopia for all age groups, except for those older than 65 years.
Conclusions: This study demonstrates age-related reduction in TISA500 and TICV500, a marker of anterior chamber depth as measured by ASOCT, in open angle eyes. This is consistent with the known shallowing of the anterior chamber with aging. This study establishes a normal age-adjusted range of TICV500, a parameter which could potentially be useful for defining criteria for intervention in narrow angles or monitoring the effects of treatment.

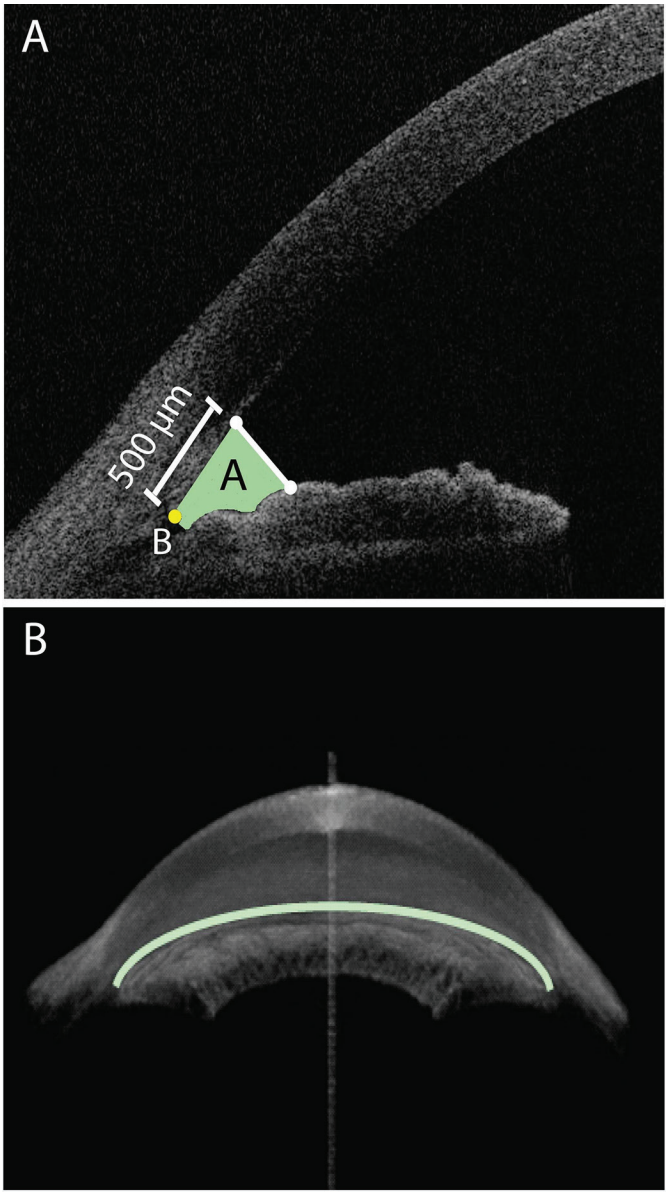

Figure 1. A) Anterior chamber angle 2D image exhibiting trabecular-iris space area (TISA) and the scleral spur landmark (SSL). Adapted with permission from Cumba et al., Journal of Ophthalmology 2012;2012:487309. B) 3D anterior chamber angle image exhibiting trabecular-iris circumference volume (TICV).

Variable	Age ≤ 35 years (N=18)	35< Age ≤ 45 (N=20)	45< Age ≤ 55 (N=17)	55< Age ≤ 65 (N=17)	Age >65 (N=18)
TISA500(mm^2)					
Temporal	0.1928 (0.0696)	0.1659 (0.0577)	0.1139 (0.0440)	0.1445 (0.0779)	0.1319 (0.0595)
Nasal	0.1952 (0.0817)	0.1719 (0.0667)	0.1197 (0.0636)	0.1563 (0.0824)	0.1469 (0.1192)
Superior	0.1571 (0.0594)	0.1339 (0.0638)	0.0712 (0.0488)	0.0881 (0.0552)	0.0934 (0.0652)
Inferior	0.2089 (0.0815)	0.1592 (0.0650)	0.1025(0.0691)	0.1262 (0.0786)	0.1285 (0.0648)
TICV500 (µl)	6.2978 (2.1972)	5.2584 (1.8416)	3.4401 (1.5683)	4.2566 (1.9846)	4.1500 (2.3195)

Table 1. Angle measurements for TISA500 and TICV500 (mean[SD])

Commercial Relationships: Mohammed Rigi, None; **Donna Nguyen**, None; **Lauren S. Blieden**, None; **Nicholas P. Bell**, None; **Laura Baker**, None; **Alice Chuang**, None; **Robert M. Feldman**, Tomey Corporation (F)
Support: NEI Vision Core Grant P30EY010608; Challenge Grant from Research to Prevent Blindness to The University of Texas Medical School at Houston; Hermann Eye Fund

Program Number: 931 **Poster Board Number:** A0283
Presentation Time: 3:15 PM–5:00 PM
Use of a Novel Anterior Segment Swept-Source Optical Coherence Tomography in Assessing Iris and Iridocorneal Angle Structures

Ahmad Najafi[1], Sung Chul Park[1, 2], Jeffrey M. Liebmann[1, 3], Robert Ritch[1, 2]. [1]Moise and Chella Safra Advanced Ocular Imaging Laboratory, New York Eye and Ear Infirmary of the Mount Sinai Health System, New York City, NY; [2]Ophthalmology, New York Medical College, New York, NY, New York City, NY; [3]Ophthalmology, New York University School of Medicine, New York City, NY.

Purpose: To test a novel high-speed, high-resolution anterior segment swept-source optical coherence tomography (SS-OCT) in assessing the iris and iridocorneal angles in different physiologic conditions.
Methods: Horizontal cross-sectional B-scans were obtained for the nasal and temporal iridocorneal angles of normal subjects using a novel anterior segment SS-OCT (Casia SS-1000; Tomey, Nagoya, Japan). Iris and iridocorneal angle structures were assessed in different positions of gaze and during accommodation.
Results: Sixteen normal eyes (8 subjects) were tested. The SS-OCT successfully imaged the cornea, iris and anterior chamber angles and provided semi-automated built-in measurement tools for those structures (Fig 1). Forward movement of the lens, changes in iris curvature, and widening of the iridocorneal angles (increase in angle opening distance [AOD] and trabecular iris angle [TIA]) during accommodation were demonstrated (Fig 1A, 1B). Changes in iridocorneal angle measurements (AOD and TIA) on abduction and adduction of the eyes were also identified (Fig 1C-1E). Regional iris length and thickness also underwent dynamic changes depending on the position of the tested eye and/or regional difference in illumination; in straight forward gaze, the tested eye became slightly adducted and the temporal iris region became longer and thinner than the nasal iris region (Fig 1F, 1G).
Conclusions: This new anterior segment SS-OCT provides high-speed, high-resolution cross-sectional images of the anterior segment structures and may be helpful in investigating and understanding subtle pupillary movement and iridocorneal angle structure changes in various conditions. Eye position relative to the light source of the OCT and accommodation may cause changes in iris and iridocorneal angle structures. A standardized protocol for testing condition is needed for reliable and accurate assessment of the anterior segment structures using SS-OCT.

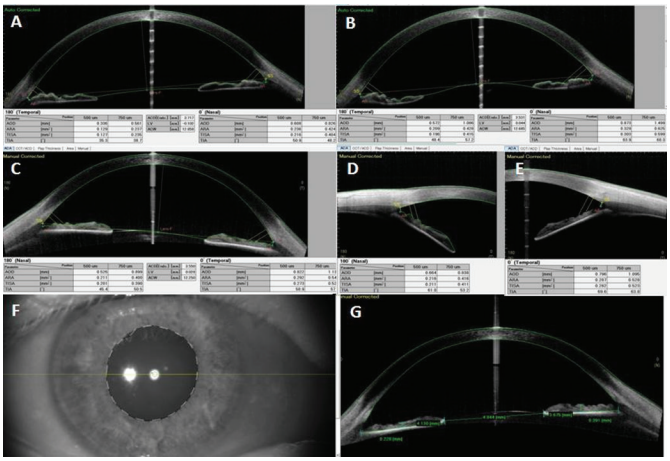

(A) Before and (B) after accommodation. (C) Straight forward gaze, (D) abduction and (E) adduction. (F) Infrared image and (G) cross-sectional SS-OCT image during straight forward gaze.

Commercial Relationships: Ahmad Najafi, None; **Sung Chul Park**, None; **Jeffrey M. Liebmann**, None; **Robert Ritch**, None

Program Number: 932 **Poster Board Number:** A0284
Presentation Time: 3:15 PM–5:00 PM
Comparison of time domain anterior segment OCT with swept source OCT for angle closure imaging

Baskaran Mani[1, 2], Christine Yau[2], Sue-Wei Ho[1], Tin A. Tun[1], Shamira Perera[1], Tin Aung[1, 2]. [1]Glaucoma, Singapore Eye Research Institute, Singapore, Singapore; [2]Ophthalmology, Yong Loo Lin School of Medicine, National University of Singapore, Singapore, Singapore.

Purpose: To compare angle closure assessed by conventional time domain anterior segment optical coherence tomography (ASOCT) using 2 scans, with swept source OCT (SSOCT) using 360° anterior segment imaging, with gonioscopy as the reference standard.
Methods: ASOCT (Visante, Carl-Zeiss Meditec, Dublin) was performed in dark conditions and 2 scans (one vertical and one horizontal) were obtained for all participants. SSOCT 3-dimensional angle scans (CASIA SS-1000, Tomey Corporation, Nagoya, Japan), that obtain 128 radial scans for the entire circumference of the angle, were performed under dark conditions. Iris Trabecular Contact (ITC) index was calculated as a percentage of the angle that was closed on 16/128 SSOCT scans using in-built customized software. Qualitative assessment of angle status was also determined for all 128 SSOCT scans. Angle closure on gonioscopy was defined as non-visibility of posterior trabecular meshwork for at least 2 quadrants. Angle status in anterior segment imaging scans was considered closed if ≥50% of the frames showed angle closure as assessed by a masked clinician. Cohen's Kappa statistics (k) and area under the receiver operating characteristic (AUC) curve analyses were performed for angle closure based on the 3 types of scan methods in comparison to gonioscopy.
Results: Study subjects (n=126, closed angles – 31, 24.6%) were predominantly Chinese (95.2%) and female (71.4%) with a mean age of 59.5 (standard deviation, SD = 8.9) years. Agreement for angle closure diagnosis based on ASOCT (2 scans, k = 0.32) vs SSOCT

16 scans (ITC index, k = 0.39) vs SSOCT 128 scans over 360° (k = 0.32) was fair in comparison to gonioscopy . AUC for gonioscopic angle closure detection was comparable for all 3 imaging methods (ASOCT 2 scans AUC 0.72, [95% CI – 0.64, 0.80], SSOCT ITC index 16 scans AUC 0.67 [95% CI – 0.58, 0.75] and SSOCT 128 scans AUC 0.69 [95% CI – 0.60, 0.76]).
Conclusions: Time domain ASOCT using 2 anterior segment scans had comparable diagnostic performance to 360° SSOCT using 16 or 128 anterior segment scans, for gonioscopic angle closure diagnosis. Both methods showed moderate agreement with gonioscopy.
Commercial Relationships: Baskaran Mani, None; **Christine Yau**, None; **Sue-Wei Ho**, None; **Tin A. Tun**, None; **Shamira Perera**, None; **Tin Aung**, None
Support: Translational Clinical Research Program grant, Biomedical Research Council (BMRC), Singapore and National Medical research Council, Singapore

Program Number: 933 **Poster Board Number:** A0285
Presentation Time: 3:15 PM–5:00 PM
Repeatability and Comparison of Anterior Chamber Angle Assessment Tests
Peter Campbell[1, 3], Rishi Agarwal[2, 3], Tony Redmond[4, 2], K Sheng Lim[1], Bruce Evans[2, 3]. [1]Ophthalmology, St Thomas' Hospital, London, United Kingdom; [2]Institute of Optometry, London, United Kingdom; [3]Faculty of Health and Social Care, London South Bank University, London, United Kingdom; [4]Cardiff Centre for Vision Sciences, School of Optometry and Vision Sciences, Cardiff University, Cardiff, United Kingdom.
Purpose: To evaluate the repeatability of gonioscopy, van Herick method and Anterior Segment Optical Coherence Tomography (AS-OCT) and assess the agreement between these techniques.
Methods: Gonioscopy, van Herick method and AS-OCT were performed on two occasions, one month apart, on patients recruited from optometry practice. All tests were undertaken by one optometrist. One eye was randomly selected for inclusion in the analysis. An eye was graded as occludable with gonioscopy if the posterior pigmented trabecular meshwork was not visible for 90 degrees or more. Anterior Segment images were captured with a Topcon OCT-2000 using the anterior segment setting (see image below). AS-OCT images were graded by a second optometrist masked to the gonioscopy and van Herick method results. The weighted kappa statistic (κ) was used to measure repeatability and agreement.
Results: Results were obtained for 80 eyes of 80 subjects. For gonioscopy, 12 subjects were found to have occludable angles on visit 1 (15%) and 13 subjects on visit 2 (16.2%), κ=0.542. For van Herick method, 17 subjects were found to have occludable angles on visit 1 (21.2%) and 12 subjects on visit 2 (15%) κ=0.641. For AS-OCT, 12 subjects were found to have occludable angles on visit 1 (15%) and 10 subjects on visit 2 (12.5%), κ=0.641. Four subjects had an occludable grading with all three methods at visit 1 and three subjects at visit 2.
The agreement between gonioscopy and van Herick was good: κ=0.641 at visit 1 and κ=0.708 at visit 2; agreement between gonioscopy and AS-OCT was fair: κ=0.546 at visit 1 and κ=0.510 at visit 2.
Conclusions: Gonioscopy, despite being a semi-subjective test, is the gold standard method for detecting primary angle closure. Intra-observer repeatability for gonioscopy, van Herick method and AS-OCT is fair, with van Herick method and AS-OCT performing better than gonioscopy. The van Herick method appears to show good agreement with gonioscopy, whereas agreement between AS-OCT and gonioscopy is fair. The van Herick method would appear to be preferable to AS-OCT when considering alternatives to gonioscopy, for example, in glaucoma shared care schemes. OCT instruments that are specifically designed for anterior segment imaging may perform better but are not widely available in clinical practice.

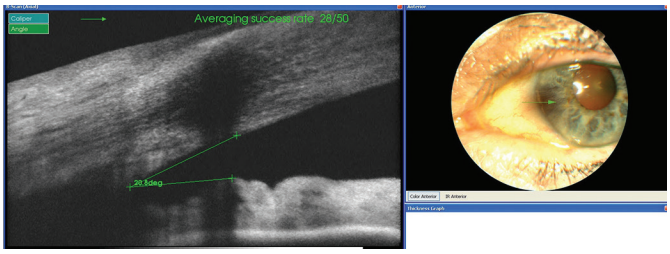

Anterior Segment OCT Image (Topcon-2000)
Commercial Relationships: Peter Campbell, College Of Optometrists (F), Topcon Great Britain Ltd (F); **Rishi Agarwal**, None; **Tony Redmond**, None; **K Sheng Lim**, None; **Bruce Evans**, None
Support: College of Optometrists, iPRO Small Grants Scheme

Program Number: 934 **Poster Board Number:** A0286
Presentation Time: 3:15 PM–5:00 PM
Anterior segment structural analysis with optical coherence tomography in primary congenital glaucoma
Rita Anjos, luisa vieira, Mariana Cardoso, Andre Vicente, Luís Pinto, Cristina Ferreira, Ana Xavier, Vitor Maduro, Cristina Brito. centro hospitalar lisboa central, Lisboa, Portugal.
Purpose: To analyse anterior segment structure using anterior segment optical coherence tomography (AS-OCT) in children with primary congenital glaucoma (PCG).
Methods: A prospective case-control study was conducted in children with PCG and without glaucoma (control group), followed in Pediatric Ophthalmology Section of Hospital Dona Estefânia, Centro Hospitalar de Lisboa Central. A complete ophthalmologic evaluation and AS-OCT (AC biometry protocol) were done.
Results: Twenty-seven eyes (17 children with PCG) and 22 eyes (11 children without glaucoma) were enrolled in this study. In PCG group were detected higher values of anterior chamber (AC) width and central depth (p<0,001), larger angle-opening distance at 500 (p<0,001) and 750μm (p=0,001), trabecular-iris space area at 500 and 750μm (p<0,001) and angle recess area at 500 (p<0,001) and 750μm (p=0,001). Iris was singificantly thinner at 500μm from the scleral spur (p=0,011), in the middle of the iris (p<0,001) and at the thickest part (p=0,001), and longer (p<0,001), in PCG group. Visual acuity (logMAR) and AC width were positively correlated (r=0,688; p<0,001). Other features found included iris hypoplasia and anterior displacement.
Conclusions: This first study in children with PCG suggests that AS-OCT is relatively easy to acquire, can help in clinical and surgical follow-up and be useful as prognostic factor.
Commercial Relationships: Rita Anjos, None; **luisa vieira**, None; **Mariana Cardoso**, None; **Andre Vicente**, None; **Luís Pinto**, None; **Cristina Ferreira**, None; **Ana Xavier**, None; **Vitor Maduro**, None; **Cristina Brito**, None

Program Number: 935 **Poster Board Number:** A0287
Presentation Time: 3:15 PM–5:00 PM
Iridocorneal angle changes measured by anterior segment optical coherence tomography in narrow angle patients after phacoemulsification with intraocular lens implantation
Jose A. Hernandez-Vargas, Jesus Jimenez-Arroyo, Mariana Escalante-Castañon, Magdalena García-Huerta, Jesus Jimenez-Roman. Glaucoma, Assoc Para Evitar la Ceguera en Mexico, IAP, Mexico, Mexico.
Purpose: Measure the iridocorneal characteristics with anterior segment optical coherence tomography before and after phacoemulsification with intraocular lens implantation in patients with cataract and narrow angle or primary angle closure glaucoma (PACG).
Methods: Prospective, longitudinal, experimental case series of patients diagnosed with cataract and narrow angle or PACG in which phacoemulsification with intraocular lens implantation was performed. Iridocorneal angle measurement was performed with anterior segment optical coherence tomography (AS-OCT RTVue Optovue, Fremont, CA, USA) before cataract surgery and after one month. The measurements with OCT were: iridocorneal angle, angle opening distance at 500 and 750 μm (AOD 500-750), trabecular-iris space area at 500 and 750 μm (TISA 500-750) and angle recess area (ARA). We also evaluated best-corrected visual acuity (BCVA), intraocular pressure (IOP) and gonioscopy with Shaffer grade system and lens opacity with LOCS III before and after phacoemulsification.
Results: We included 12 eyes (10 patients), 12 were female (100%), mean age of 74.67 years (± 6.41), 9 patients diagnosed with narrow angle and 3 with PACG. Before surgery we found a mean BCVA in LogMAR 0.34 (± 0.10), refraction of +2.39 (± 2.13), Shaffer grade system between 0-2 and antero-posterior axis of 22.66 (± 0.81). In the measurements made by OCT: iridocorneal angle, AOD 500-750, TISA 500-750 and ARA after phacoemulsification we found a statistically significant ($p<0.05$) increase that correlated with gonioscopy (Shaffer 2-4). IOP was not significantly changed before and after phacoemulsification in any patients.
Conclusions: Phacoemulsification with intraocular lens implantation significantly modifies iridocorneal angle anatomy, increasing its dimensions. The OCT is a noncontact instrument that allows us to analyze these changes objectively. Studies with longer follow-up are needed to confirm our long-term results.
Commercial Relationships: Jose A. Hernandez-Vargas, None; **Jesus Jimenez-Arroyo**, None; **Mariana Escalante-Castañon**, None; **Magdalena García-Huerta**, None; **Jesus Jimenez-Roman**, None

Program Number: 936 **Poster Board Number:** A0288
Presentation Time: 3:15 PM–5:00 PM
Anterior chamber biometrics and intraocular pressure dynamics following cataract extraction in glaucoma patients
Ferhina S. Ali[1], Sasan Moghimi[1], Diego T. Barbosa[1], Guofu Huang[2], Shan C. Lin[1]. [1]Ophthalmology, University of California San Francisco, San Francisco, CA; [2]Ophthalmology, Nanchang Eye Hospital, Nanchang, China.
Purpose: To determine the association of changes in anterior chamber biometrics and intraocular pressure after uncomplicated phacoemulsification in patients with primary open angle glaucoma.
Methods: In this prospective study, subjects with medically managed glaucoma underwent phacoemulsification with implantation of a foldable lens. Preoperatively and postoperatively, anterior chamber parameters were obtained by anterior segment coherence tomography. Measurements included the angle opening distance 500 μm anterior to the scleral spur (AOD500), the trabecular–iris space area 500 μm (TISA500) from the scleral spur, and iris curvature (I-Curv).
Results: Data was analyzed from 34 glaucomatous eyes that underwent cataract surgery. The mean patient age was 77 years ± 7.39 (SD); 67% of the patients were women. On average, the patients were being treated with 1.77 (0.8) glaucoma medications. From preoperative to postoperative time points, the mean (SD) AOD 500 increased significantly by 0.180 mm (0.133) and the mean TISA 500 increased with marginal significance by 0.054 mm3 (.050). The mean IOP (SD) decreased significantly from 14.26 (4.029) to 11.73 (3.355) with a mean difference of -2.535 (4.214); $p < 0.01$. This change in intraocular pressure correlated by marginal significance with the increase in the AOD 500 ($r=0.30$, $p=0.05$) and with iris curvature ($r=-0.032$, $p=0.05$).
Conclusions: These findings provide additional etiologic basis for the postoperative reduction in intraocular pressure that is observed in glaucoma patients following cataract surgery. The reduction in IOP was proportional to the increase in the angle opening and iris curvature observed following cataract surgery. This study further establishes a role for consideration of cataract surgery in the treatment algorithm of primary open angle glaucoma.
Commercial Relationships: Ferhina S. Ali, None; **Sasan Moghimi**, None; **Diego T. Barbosa**, None; **Guofu Huang**, None; **Shan C. Lin**, None
Support: Core grant EY002162 from the National Eye Institute; Research to Prevent Blindness Foundation; That Man May See, Inc.; National Natural Science Foundation of China (Grant No.81260147)

Program Number: 937 **Poster Board Number:** A0289
Presentation Time: 3:15 PM–5:00 PM
Effect of Angle of Incidence on Anterior Chamber Angle Metrics from Optical Coherence Tomography
Jyotsna Maram, Xiaojing Pan, Ken Marion, Zhou Y. Zhang, Srinivas R. Sadda, Vikas Chopra. Ophthalmology, Doheny Eye Institute, Los Angeles, CA.
Purpose: To evaluate the local variability of anterior chamber angle (ACA) metrics obtained by time domain (TD) and spectral domain (SD) optical coherence tomography (OCT).
Methods: Anterior segment OCT imaging was performed on 30 normal eyes using Visante TD-OCT and on 40 normal eyes using Cirrus SD-OCT. For Visante OCT, a single 16-mm line scan of the inferior angle with three slightly different rotations of 265, 270 and 275 was performed. For Cirrus OCT, a 5-line raster of the inferior angle was performed, centering the third scan line at the 6 o'clock position, with 0.25 mm between lines. ACA measurements were taken for angle opening distance (AOD) and trabecular iris space area (TISA) at 500/750 μm from the scleral spur for Visante OCT and at Schwalbe's line (SL) for Cirrus OCT. Measurements between line scans for each device were compared and quantified.
Results: For the Visante OCT at three different scan orientations, the mean difference in ACA metrics was 0.41±0.15 mm for AOD-500, 0.59±0.22 mm for AOD-750, 0.14±0.06 mm2 for TISA-500, and 0.27±0.1 mm2 for TISA-750. For three different scan positions with Cirrus OCT, the AOD-SL and TISA-SL showed mean differences of 0.85±0.32 mm and 0.33±0.15 mm2, respectively.
Conclusions: These findings suggest that small local changes in the position of the OCT line scan did not significantly alter ACA metrics in achieving reliable measurements. Given the absence of tracking and registration for current anterior segment OCT instruments, this observation is of relevance for longitudinal and dynamic studies of angle geometry.

Commercial Relationships: Jyotsna Maram, None; **Xiaojing Pan**, None; **Ken Marion**, None; **Zhou Y. Zhang**, None; **Srinivas R. Sadda**, Allergan (C), Carl Zeiss Meditec (C), Carl Zeiss Meditec (F), Genentech (C), Optos (C), Optos (F), Optovue (F), Regeneron (C); **Vikas Chopra**, Allergan (C)

Program Number: 938 **Poster Board Number:** A0290
Presentation Time: 3:15 PM–5:00 PM
The compatibility of the location of scleral spur in the observation of anterior segment optical coherence tomography and histological examination
Teruhiko Hamanaka[1], Tomohiko Higashida[1], Tetsuro Sakurai[2], Nobuo Ishida[3]. [1]Ophthalmology, Japanese Red Cross Medical Ctr, Shibuya-Ku, Japan; [2]Center of Education, Tokyo University of Science, Suwa, Japan; [3]Ishida Eye Clinic, Joetsu, Japan.
Purpose: Angle-structure data obtained by anterior segment optical coherence tomography (AS-OCT) plays an important role for evaluating the risk for primary angle-closure glaucoma (PACG). For angle-structure evaluation, scleral spur (SS) is a fundamental point for various parameters; e.g., angle opening distance (AOD) and trabecular-iris space area (TISA). However, SS in AS-OCT images is mostly unclear and difficult to detect. In this study, we evaluate the compatibility in the detection of SS observed by AS-OCT and histological examination of trabeculectomy (TLE) specimens.
Methods: Angle structure images were obtained from 38 open-angle glaucoma eyes and 12 angle-closure glaucoma eyes pre and post TLE by AS-OCT (Visante OCT; Carl Zeiss Meditec, Dublin, CA, Casia SS-1000, Tomey Corp., Nagoya, Japan). TLE specimens were embedded in paraffin and processed for hematoxylin-eosin (HE), Masson trichrome, and thrombomodulin immunohistochemical staining. Locations of bottom of the angle recess (BAR) and SS (on the border line of ciliary body and sclera) were input on the printed AS-OCT image (Figure. SS: arrowhead, BAR: arrow; top left inset). On the histological image, the location of Schwalbe's line (SW) (Figure, solid arrowhead), SS (Figure, open arrowhead), BAR (Figure, arrow), and anterior and posterior tips of the Schlemm's canal (SC) (Figure) were also input, and then the distance of SW-SS and SS-BAR were measured. SS defined to input the most bulging part of SS. The development of SS was categorized into 4 grades [grades 0 (less) to III (prominent)]. All histological images were inserted into the defective area of the post-TLE AS-OCT images (Figure, top right inset).
Results: All SS on the AS-OCT images were located 218±147μm (mean±SD) posterior to BAR. On the histological images, SS was located anteriorly (50%) and posteriorly (50%) to BAR (6±98μm). The distance between SW and SS was 612±83μm. The length of SC was 233±61μm. The ratio of the development grades of SS were as follows: 0: 25%, I: 50%, II: 9%, III: 16%). The development of SS was significantly correlated with SS-BAR.
Conclusions: SS could not be precisely detected by any type of AS-OCT, and SS on AS-OCT images tended to be input more posteriorly to BAR. The angle recession, which indicates BAR, may be located more posteriorly in eyes with developed SS.

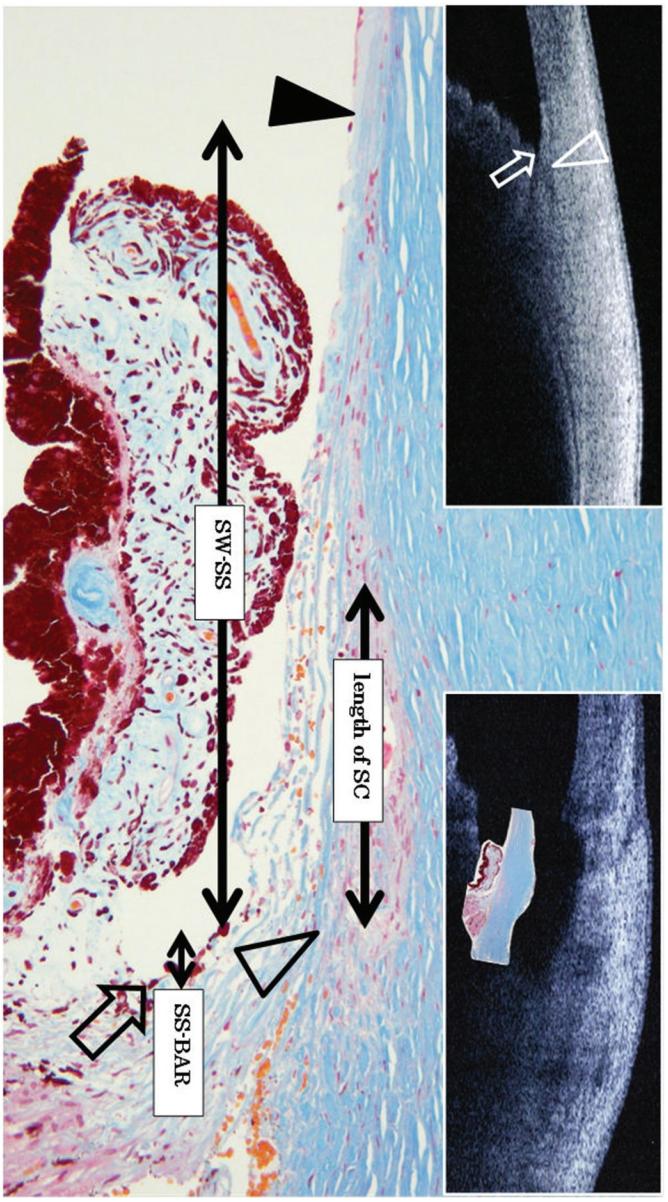

Commercial Relationships: Teruhiko Hamanaka, None; **Tomohiko Higashida**, None; **Tetsuro Sakurai**, None; **Nobuo Ishida**, None

Program Number: 939 **Poster Board Number:** A0291
Presentation Time: 3:15 PM–5:00 PM
A 3-year prospective analysis of anterior chamber depth using the swept-source optical coherence tomography
Heather K. Mak, Christopher K. Leung. Ophthalmology and Visual Sciences, The Chinese University of Hong Kong, Hong Kong, Hong Kong.
Purpose: To measure the longitudinal changes in the anterior chamber depth (ACD) and angle width using a swept-source anterior segment optical coherence tomography (OCT) and investigate factors associated with the change in ACD over three years of follow-up.
Methods: A total of 42 eyes from 38 primary open-angle glaucoma patients followed for ≥3 years were analyzed. All eyes were phakic during the follow-up. The anterior segment was imaged by a swept-source anterior segment OCT (Casia SS-1000 OCT, Tomey, Nagoya,

Japan) in the dark at the baseline and then in 3 years. ACD and angle width of the horizontal meridian were measured using the instrument software. Linear mixed models were used to examine the association between the change in anterior chamber depth and age, gender, axial length, pupil diameter change, and angle width parameters (angle opening distance, trabecular iris space area, and trabecular iris area).
Results: The mean age, ACD, axial length, and angle opening distance at final visit were 51.3 years, 2.8mm, 24.9mm and 547.6μm, respectively. The mean ACD significantly decreased after three years (mean±SD: -34.6±7.8μm, p<0.001), but there were no significant changes in the angle width. The change in ACD was negatively associated with age (p=0.043). A younger age had a larger change in ACD. There were no significant associations between change in ACD and gender, axial length, or angle width parameters (p>0.082).
Conclusions: The mean ACD decreased with age, suggesting an anterior displacement of the anterior lens surface over time. Change in ACD was more obvious in patients with a younger age.

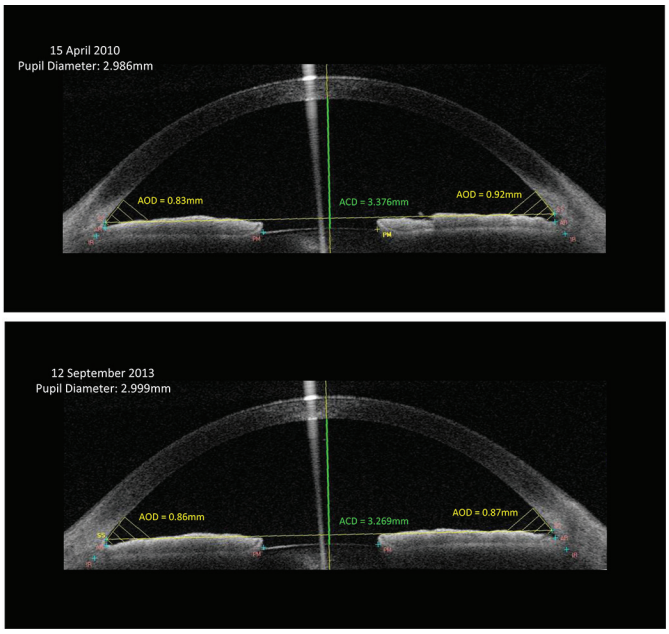

An example of a 49 year-old man illustrating the change in anterior chamber depth from baseline to final visit (41 months).
Commercial Relationships: Heather K. Mak, None; **Christopher K. Leung**, Tomey (F)

Program Number: 940 **Poster Board Number:** A0292
Presentation Time: 3:15 PM–5:00 PM
Evaluation and Comparison of Novel Anterior Chamber Angle Metrics Using Two Spectral Domain OCT Devices
Moritz Niemeyer[1], Ken Marion[1], Srinivas R. Sadda[1, 2], Vikas Chopra[1, 2]. [1]Doheny Imaging Reading Center, Doheny Eye Institue, Los Angeles, CA; [2]Department of Ophthalmology, Keck School of Medicine, University of Southern California, Los Angeles, CA.
Purpose: To compare novel Schwalbe's line-based anterior chamber angle parameters obtained from two widely-available spectral domain optical coherence tomography (SD-OCT) instruments, and to evaluate the reproducibility of these metrics in normal and glaucomatous eyes.
Methods: Inferior irido-corneal angles of 95 eyes from 51 participants (30 Glaucoma and 21 normal) were scanned twice with the Optovue SD-OCT and Cirrus SD-OCT under controlled low luminance conditions. Novel metrics termed the Schwalbe's line angle opening distance (SL-AOD) and SL trabecular-iris-space area (SL-TISA) were graded by masked certified graders at the Doheny Imaging Reading Center using customized Image J software. Inter-instrument agreement and inter-grader reproducibility of SL-AOD and SL-TISA measurements were evaluated by intra-class correlation coefficients (ICC), mean percent difference (MPD), and coefficient of variability (CV).
Results: The mean SL-AOD for the total study cohort was 587 μm+/-247 μm (range 142-1121μm) for the Optovue and 596 μm+/-278 μm (122-1257 μm) for the Cirrus. The mean SL-TISA was 204.4 μm2+/-99.1μm2 (423.0-447.1 μm2) for the Optovue and 210.0μm2+/-107.2μm2 (33.7-497.7 μm2) for the Cirrus. The measurements between devices were highly correlated for both SL-AOD (R2=0.928, intraclass correlation coefficient (ICC) = 0.952) and SL-TISA (R2=0.867, ICC = 0.963) The mean percentage differences between the SD-OCT devices for the SL-AOD and SL-TISA measurements were 2.1% and 2.3% respectively, with coefficients of variation (CV) of 1.0 and 1.0, respectively. Inter-grader agreement was excellent for both devices, for both SL-AOD (CV= 1.3 Cirrus, CV=1.2, Optovue) and SL-TISA (CV= 1.2, Cirrus, CV=1.2, Optovue). No differences in inter-instrument or inter-grader agreement were observed between normal and glaucomatous eyes.
Conclusions: Novel Schwalbe's line-based angle metrics showed excellent agreement between two different SD-OCT devices and between graders. These findings are promising for the use of these parameters in clinical studies, and suggest that multiple SDOCT devices may be used in the context of the same trial.
Commercial Relationships: Moritz Niemeyer, None; **Ken Marion**, None; **Srinivas R. Sadda**, Allergan (C), Carl Zeiss Meditec (C), Carl Zeiss Meditec (F), Genentech (C), Optos (C), Optos (F), OptoVue (F), Regeneron (C); **Vikas Chopra**, Allergan (C)

Program Number: 941 **Poster Board Number:** A0293
Presentation Time: 3:15 PM–5:00 PM
PROSPECTIVE SWEPT SOURCE OPTICAL COHERENCE TOMOGRAPHY ANALYSIS OF EARLY CILIOCHOROIDAL DETACHMENT IN GLAUCOMA SURGERY
Aritz J. Urcola[1, 2], Cristian Dalmasso[1], Javier Cabrerizo[1], Gonzaga Garay[1], Itziar Ozaeta[1]. [1]Ophthalmology, Hospital Universitario Araba, Vitoria-Gasteiz, Spain; [2]Universidad del País Vasco, Vitoria-Gasteiz, Spain.
Purpose: To determine the presence and relationship between annular cilichoroidal detachment (CCD) and early postoperative intraocular pressure (IOP) in non penetrating deep sclerectomy (NPDS) glaucoma surgery.
Methods: Prospective, observational non-comparative study over thirty two eyes of 32 patients that underwent NPDS. All surgeries were performed with intraoperative antimetabolite agent (mitomycin c 0.2 mg/ ml) and without any intraescleral implant. Patients were examined at 24 hour, 1, 2, 3, 4 and 8 week postoperative follow-up visits by goldman tonometer IOP and swept source optical coherence tomography (SS-OCT). Standarized four sclerolimbar quadrants were analyzed in each visit to detect annular ciliochoroidal detachment with SS-OCT (SS-1000 CASIA; Tomey, Nogoya, Japan).
Mean postoperative IOPs were compared between eyes with and without CCD in each visit. Resolution time of CCD reattachment and correlation with factors as: gender, age, type of surgery and corneal pachymetry was also studied.
Results: The incidence of CCD was 53.1% (17 eyes) in the first 24 hour and decreased progressively to 25% (8 eyes) and 6.2% (2 eyes) in 2 week and 4 week examination respectively. The mean postoperative IOPs were significantly lower ($p < 0.05$) in eyes with annular CCD comparing to eyes without in the 1 and 2 week follow-

up (9.6 mm Hg Vs 12.8 mm Hg and 9.0 mm Hg Vs 12.4 mm Hg respectively). Mean period of CCD resolution was 17.2 days (range 3-59 days). In the multivariate analysis a thinner central corneal thickness was the only factor associated to higher incidence of CCD.
Conclusions: SS-OCT technology is a non invasive diagnostic tool apropppriate to monitor presence of annular ciliochoroidal detachment postperatively. Ciliochoroidal detachment was present in 53% of NPDS surgeries in the early postoperative visit. Presence of annular CCD is related with lower postoperative IOP in the first 2 weeks follow-up

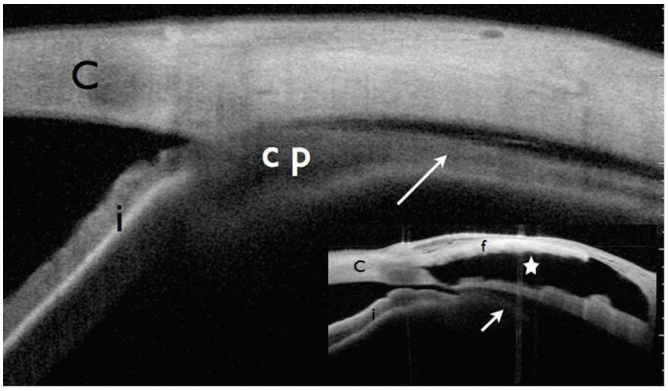

Temporal scleral radial scan showing ciliochoroidal detachment (arrow) in the 24 hour visit
Below: Superior radial scan showing large intrascleral lake (asterisk)
C: Cornea, i: Iris, cp: cilliary process, f: superficial scleral flap

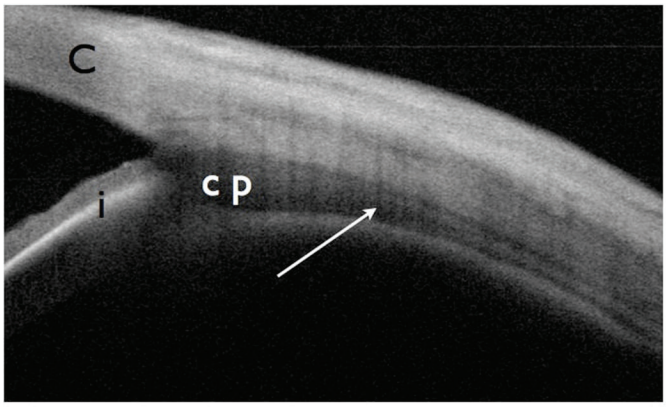

Temporal radial scan showing ciliochoroidal reattachment at 2 week postoperative visit
C: Cornea, i: Iris, cp: cilliary process
Commercial Relationships: Aritz J. Urcola, None; **Cristian Dalmasso**, None; **Javier Cabrerizo**, None; **Gonzaga Garay**, None; **Itziar Ozaeta**, None
Support: Gobierno Vasco / Eusko Jaurlaritza (2011111135)

Program Number: 942 **Poster Board Number:** A0294
Presentation Time: 3:15 PM–5:00 PM
Anterior segment OCT and confocal microscopy can be predictive of the bleb failure of a new minimally invasive glaucoma surgery technique, the XEN implant (Aquesys)?
Giulia Consolandi, Antonio M. Fea, Carlo Alessandro Lavia, Giulia Pignata, Paola Maria Loredana Cannizzo, Francesco Gallozzi, Roberta Spinetta, Teresa Rolle, Federico M. Grignolo. Università degli Studi di Torino, Torino, Italy.
Purpose: Most of the minimally invasive glaucoma surgery (MIGS) procedures address the angle or the suprachoroidal space by the use of new implants (Glaukos, Ivantis, Transcend, MidiArrow) but their proper placement and the patency of the outflow pathways remains a matter of clinical experience. Aim of the study was to investigate if anterior segment OCT and confocal microscopy could add clinical informations of the long term health of the bleb obtained using a new collagen derived implant (XEN).
Methods: The device was implanted in 10 POAG patients (8 males/ 2 females, 64,5 mean age ±12,93 SD). IOP with GAT, AS-OCT (RTVue, Optovue), confocal microscopy (Heidelberg) were assessed one day, 1 week, 1 month and 6 months post-operatively. At the same time points, bleb morphology was evaluated by two masked observers. The bleb was defined as present, encapsulated, cystic or absent. The position and the presence of fluid were evaluated using the AS-OCT. The presence of subconjunctival cystic spaces was assessed by the confocal microscopy. Complete success was defined as mean diurnal IOP<18 mm Hg and qualified success as mean diurnal IOP<18 mm Hg on medication.
Results: Direct communication between the anterior chamber and the subconjunctival space was demonstrated in all patients intraoperatively by obtaining a bleb after intracameral injection of BSS. Mean IOP 1 day post-operatively was 14 mmHg (17 mmHg less than pre-operatively medicated IOP). The bleb was defined as present in all patients at 1 month by both observers. The track of the implant could be visualized using the AS-OCT . Subconjunctival fluid on OCT (fig.1) and cystic spaces on confocal microscopy could be demonstrated in 8 and 4 patients respectively at 1 month (fig.2). The 6 patients in which there was no evidence of subconjunctival cystic spaces at one month (fig 5), failed at 6 months.
Conclusions: This new MIGS implant present the advantage of allowing direct intraoperative assessment of the outflow from the anterior chamber to the subconjunctival space. AS OCT can be used in the immediate post-operative period to determine the correct position of the implant and the presence of subconjunctival fluid. The presence of conjunctival cysts assessed by confocal microscopy seems a predictive factor of medium term failure of the bleb.

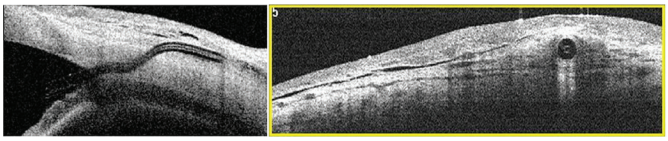

Fig. 1.

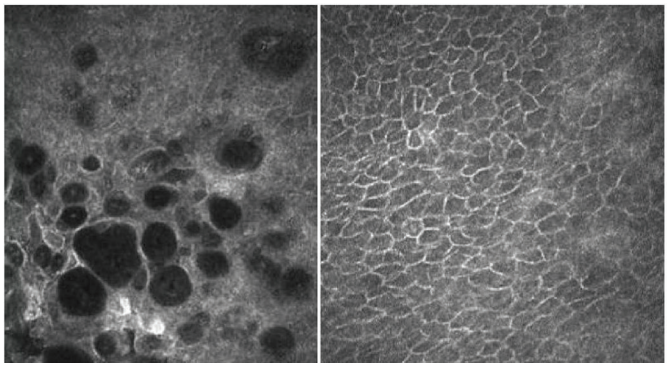

Fig. 2.
Commercial Relationships: Giulia Consolandi, None; **Antonio M. Fea**, None; **Carlo Alessandro Lavia**, None; **Giulia Pignata**, None; **Paola Maria Loredana Cannizzo**, None; **Francesco Gallozzi**, None; **Roberta Spinetta**, None; **Teresa Rolle**, None; **Federico M. Grignolo**, None

Program Number: 943 **Poster Board Number:** A0295
Presentation Time: 3:15 PM–5:00 PM
Evaluation of Bleb Birefringence after Glaucoma Surgery using Anterior Segment Polarization-Sensitive Optical Coherence Tomography
Shinichi Fukuda[1, 2], Simone Beheregaray[1, 2], Deepa Kasaragod[2, 3], Kotaro Ishii[1], Yoshiaki Yasuno[2, 3], Tetsuro Oshika[1, 2]. [1]Ophthalmology, Tsukuba University, Tsukuba, Japan; [2]Computational Optics and Ophthalmology Group, Tsukuba, Japan; [3]Computational Optics Group, Tsukuba University, Tsukuba, Japan.
Purpose: Anterior segment optical coherence tomography (OCT) can offer important morphological information regarding the bleb function after trabeculectomy and Ex-Press Tube Shunt. However, evaluation of tissue property such as fibrosis of blebs is difficult with the conventional OCT. Polarization-sensitive OCT (PS-OCT), which is a variant of functional extensions of OCT, can improve the image contrast of OCT by measuring birefringence of biological fibrous tissues. We evaluated the birefringence of trabeculectomy and Ex-Press tube shunt blebs using anterior segment PS-OCT.
Methods: Thirty eight eyes of 30 patients with glaucoma were included. There were 18 men and 12 women, with mean age of 72.4 ± 8.5 years. Of 38 eyes, 17 (44.7%) had primary open-angle glaucoma, 7 (18.4%) had primary angle-closure glaucoma, 13 (34.2%) had pseudoexfoliation glaucoma, and 1 (2.6%) had secondary glaucoma. A custom-made three-dimensional anterior segment PS-OCT built by Computational Optics Group, University of Tsukuba was utilized in this study. The system is also based on a swept-source OCT technology, and the light source was a 30,000 Hz wavelength sweeping laser which sweeps over 110 nm across a center wavelength of 1.3 μm. Blebs were scanned with a horizontal-fast raster pattern on scanning ranges of 12 × 12 mm2, including 512 horizontal × 128 vertical A-lines.
Results: The intraocular pressure (IOP) was higher than 21mmHg in 3 eyes (7.9%), lower or equal to 21mmHg with eye drops in 24 eyes (63.1%), and lower or equal to 21mmHg without eye drops in 11 eyes (28.9 %). In the high IOP group that we consider as non-functioning blebs, the area above the sclera flap displayed abnormal birefringence. According to the general anatomy of a bleb, the tissue above a normal bleb should be conjunctiva and Tenon's capsule that should not possess birefringence. Hence the phase retardation image in high IOP group indicates abnormal birefringence. On the other hand, phase retardation image of the bleb in the low IOP without eye drops group that we consider as a functioning bleb showed no abnormal birefringence inside of bleb.
Conclusions: It was suggested that PS-OCT is a useful tool for the detailed evaluation of blebs after trabeculectomy and Ex-Press tube shunt surgery by giving information about birefringence and fibrotic changes of the bleb tissues.
Commercial Relationships: Shinichi Fukuda, None; **Simone Beheregaray**, None; **Deepa Kasaragod**, Tomey (F); **Kotaro Ishii**, None; **Yoshiaki Yasuno**, Tomey (F), Tomey (P); **Tetsuro Oshika**, Tomey (F)

Program Number: 944 **Poster Board Number:** A0296
Presentation Time: 3:15 PM–5:00 PM
Prospective investigation of filtering bleb by three-dimensional anterior-segment optical coherence tomography
Toshihiro Inoue, Sachi Kojima, Ayako Fukushima, Nakashima Kei-Ichi, Hidenobu Tanihara. Department of Ophthalmology, Kumamoto Univ, Faculty of Life Sci, Kumamoto, Japan.
Purpose: To evaluate the time-dependent changes of the filtering bleb using three-dimensional anterior-segment optical coherence tomography (3D AS-OCT).
Methods: In this prospective study, we investigated the postoperative intraocular pressure (IOP) and bleb parameters including total bleb height, fluid-filled cavity height, bleb wall thickness, bleb wall intensity, and location of the filtration opening on the scleral flap 0.5, 3, 6 and 12 months after fornix-based trabeculectomy with the aid of 3D AS-OCT and custom software. Patients with neovascular glaucoma, trabeculectomy combined with other ocular surgeries and a history of ocular surgeries except phacoemulsification were excluded.
Results: Thirty-nine patients were enrolled and 30 patients completed 1-year investigations and were analyzed. Among the bleb parameters, IOP ($P = 0.001$), the number of eye drops ($P = 0.045$), and the distance from the top of the scleral flap to the filtration opening ($P = 0.001$) were significantly higher and the width of the filtration opening ($P = 0.001$) was significantly lower at 12 months than at 0.5 months after trabeculectomy. The fornix-side edge of the filtration opening shifted towards limbus ($P = 0.006$), while the limbal-side edge of it did not present significant shift between 0.5 and 12 months after trabeculectomy. Moreover, the width of the filtration opening at 0.5 months was significantly correlated with the IOP at 3 months ($P = 0.004$).
Conclusions: The location of the filtration opening on the scleral flap of the filtering bleb was firstly reported to change in a time-dependent manner after trabeculectomy. The width of the filtration opening at 2 weeks after trabeculectomy may be a prognostic factor of IOP at 3 months.
Commercial Relationships: Toshihiro Inoue, None; **Sachi Kojima**, None; **Ayako Fukushima**, None; **Nakashima Kei-Ichi**, None; **Hidenobu Tanihara**, None
Support: JSPS KAKENHI Grant Numbers 23390403, 23659814 and 23791994